CYCLOTRON RESEARCH

UNIVERSITY OF WASHINGTON

ANNUAL PROGRESS REPORT 1961

U. S. ATOMIC ENERGY COMMISSION
CONTRACT A.T. (45-1)-1388

UNIVERSITY OF WASHINGTON

Department of Physics

Cyclotron Research

PROGRESS REPORT FOR YEAR ENDING JUNE 15, 1961

PROGRAM "A"--EXPERIMENTAL PHYSICS PROGRAM (CYCLOTRON)

UNDER

U.S. ATOMIC ENERGY COMMISSION CONTRACT A.T. (45-1)-1388

PREFACE

This report is a review of the research and technical developments conducted at the 60-inch cyclotron at the University of Washington during the year ending June 15, 1961.

Considerable effort has been devoted during the past year to the development of new experimental facilities. Investigations described in this report which particularly involve recently completed tools include: the study of the C^{10}-Be^{10} coulomb energy difference, using the "orange" spectrometer to measure the beta-ray end-point energy; studies of inelastic alpha particle scattering using solid state detectors and the heavy particle magnetic spectrometer; studies of neutron evaporation spectra using a beam deflection system in time-of-flight measurements; studies of (α, d) and $(\alpha, 2p)$ reactions using new particle identification arrangements; and p-γ and α-γ coincidence studies which are made possible by the new dee voltage regulator. A more comprehensive list of the topics studied is given in the Table of Contents.

Research at this laboratory is performed by the staff members and graduate students of the Departments of Physics and Chemistry of the University of Washington. At present, the support for this project is provided by the state of Washington and the Atomic Energy Commission.

Except for minor changes, the arrangement of the sections of this report follows the pattern used in previous years. The sections are numbered consecutively through the report; each table and figure is assigned the number of the section to which it pertains.

TABLE OF CONTENTS

I. BETA AND GAMMA RAY SPECTROSCOPY

1. Introduction

Because of construction work on the second floor of the cyclotron laboratory during the past year, and the consequent disruption of the beta-ray spectroscopy laboratory housed on this floor, considerable effort has been devoted to the permanent installation of the beta-ray spectroscopy apparatus in its newly finished quarters; Sec. 2 gives some of the details of this work. However, during this year the 38-sector "orange" spectrometer has been completed and successfully operated in the 60-inch scattering chamber. More information on this instrument appears in Sec. 3. Research with this instrument, designed to study short period beta-ray activities, has begun with an investigation of the decay of C^{10}. Three experiments discussed in the previous report[1] have been completed and their results published: the measurement by means of Bhabha scattering of the longitudinal polarization of O^{14} positrons;[2] the investigation of the decay[3] of Ag^{104}; and the precision determination of the O^{14} half life.[4]

---

1 Cyclotron Research, University of Washington (1960), p. 1,2,3.
2 J. C. Hopkins, J. B. Gerhart, F. H. Schmidt and J. E. Stroth, Phys. Rev. 121, 1185 (1961).
3 H. Nutley and J. B. Gerhart, Phys. Rev. 120, 1815 (1960).
4 D. L. Hendrie and J. B. Gerhart, Phys. Rev. 121, 846 (1961).

---

2. Equipment for the Beta-Ray Spectroscopy Laboratory

In 1958 the uniform-field beta-ray spectrometer was moved from its original location in Physics Hall to quarters in the unfinished second floor of the cyclotron laboratory. At that time the spectrometer and its associated equipment were set up temporarily so that operation could continue until final building construction was finished. During the past year while construction was being completed, it was necessary to dismantle completely the experimental equipment of the laboratory. Work on the permanent installation of the spectrometer equipment in the now completed laboratory is still in progress.

Among the alterations and improvements for the spectrometer have been complete rewiring of all electrical lines to the spectrometer, permanent installation of vacuum pumps, vacuum lines, and cooling water lines; and redesign of the interlock system and the current regulation system. In addition, the apparatus for handling active gases has been moved to the spectroscopy laboratory and made substantially more versatile.

It is expected that this work will soon be completed, and that experiments with the spectrometer will be resumed in June, 1961. (J. B. Gerhart, J. Heagney, and G. Sidhu)

3. The 38-Sector "Orange" Spectrometer

The 38-sector "orange" spectrometer described in several previous progress reports[1] has been set up in the cyclotron scattering laboratory so that it can be used to study short-period activities produced in the 60-inch scattering chamber. The spectrometer also can be operated independently of the cyclotron for test purposes in a neaby area. With the present baffle system the spectrometer has a resolution of 2.1 per cent and a transmission greater than 1.5 per cent for a 5/16" by 1/4" source. The b-value of the spectrometer,[2] essentially the momentum-to-current ratio for focussed electrons, is 1.0, an unusually large value for spectrometers of this type. (F. J. Bartis and F. H. Schmidt)

---

1 Cyclotron Research, University of Washington (1957) p. 2; (1959) p. 7; (1960) p. 45.
2 O. Kofoed-Hansen, J. Lundhard, and O. B. Nielsen, Dan. Mat. Fys. Medd., 25, no. 16 (1950).

---

4. The 4.1 Mev Positron Spectrum of the O^{14} Beta-Decay

Before the start of construction in the beta-ray laboratory preliminary runs were completed in which the O^{14} beta-ray spectrum was observed with the uniform field spectrometer. The internal spectrometer source, cooled with liquid nitrogen, was operated satisfactorily, and the source monitoring system was partially tested. Positrons from the weak high-energy O^{14} transition were easily detected with a geiger counter in the presence of the gamma-ray background from the source. Work on this experiment will continue when the spectrometer laboratory modifications are completed. (J. B. Gerhart, J. Heagney, F. H. Schmidt, G. Sidhu)

5. The Study of Positron Polarization by Bhabha Scattering

Because of the construction program discussed above and the departures of Dr. Hopkins and Mr. Stroth, the experiment to determine the longitudinal polarization of Co^{56} positrons has been discontinued. (J. B. Gerhart, F. H. Schmidt, and J. E. Stroth)

6. The C^{10}-Be^{10} Coulomb Energy Difference

The new "orange" spectrometer has been used to determine a tentative end-point of 1.86 ± 0.05 Mev for the higher energy branch in the C^{10} beta-decay. C^{10} was produced by the reaction $B^{10}(p,n)\ C^{10}$, with a 96 per cent B^{10} pressed powder target mounted in the 60-inch scattering chamber. In the measurement the following procedure was used: The target was bombarded for about 15 seconds; then for an equal period its beta-activity was examined with the orange spectrometer and a monitor scintillation counter; next the counting equipment was turned off. This cycle was repeated until sufficient data had been accumulated. The monitor counter recorded only the beta-activity above 1 Mev. The experimental spectrum was normalized by the monitor counter. After the data had been suitably corrected for background and for the presence of some high energy activity from a target contaminant, Fermi-Kurie plots were constructed.

This endpoint determination, together with previous data on the mass 10 nuclei[1], leads to a Coulomb energy difference of 4.61 ± 0.05 Mev between C^{10} and Be^{10}. In turn, on the basis of the harmonic oscillator shell model[2] of the nucleus this Coulomb difference was used to calculate the rms charge radii of C^{12} and Be^{9}. The results are shown in Table 6 together with the measurements that have been made by electron scattering at Stanford and interpreted with the same form of charge distribution as predicted by the shell model.[3]

Table 6. Root-Mean-Square Charge Radii

Nucleus	$\langle r^2 \rangle^{1/2}$ (Assuming j-j Coupling)	$\langle r^2 \rangle^{1/2}$ (Assuming L-S Coupling)	$\langle r^2 \rangle^{1/2}$ Stanford result[3]
C^{12}	2.30 fermis	2.41 fermis	2.41 fermis
Be^{9}	2.29 fermis	2.32 fermis	2.26 fermis

However, if the Coulomb difference between C^{10} and Be^{10} is estimated on the basis of the cluster model[4] of Wildermuth and Kanellopoulos, a serious discrepancy arises. The cluster model pictures the 1.74 Mev state of B^{10} and the ground states of C^{10} and Be^{10} as a di-nucleon cluster plus a Be^{8} cluster. This assignment helps to explain the $Li^{6}(Li^{7},t)\,B^{10}$ scattering results[5]. According to this version of the cluster model the di-nucleon should be a very large structure. In order to estimate its size, we have chosen Li^{6}, where a long-tailed charge distribution of $\langle r^2 \rangle^{1/2} = 2.80$ fermis has been reported by Meyer-Berkhout[3]. The large size of the deuteron cluster in Li^{6} has been cited by Wildermuth and Kanellopoulos in explaining this result. After expansion of the cluster model wave functions of C^{10} or Be^{10} into shell model wave functions[6] the Coulomb energy difference between C^{10} and Be^{10} was evaluated[7] with the tables of Unna[8] and an approximate method of calculation suggested by Thieberger[9]. The resulting estimate of 3.5 Mev for the Coulomb difference, when compared with the experimental value 4.61 Mev, clearly indicates that the di-proton cluster in C^{10} is not an abnormally extended charge distribution. In general, we must conclude that, if nuclei have a cluster structure, the cluster model herein discussed does not consistently describe the special properties of these clusters. (F. J. Bartis and F. H. Schmidt)

1 F. Ajzenberg-Selove and T. Lauritsen, Nucl Phys. 11, 72 (1959).
2 B. C. Carlson and I. Talmi, Phys. Rev. 96, 436 (1954).
3 V. Meyer-Berkhout, K. W. Ford and A. E. S. Green, Annals of Phys. 8, 119 (1959).
4 K. Wildermuth and Th. Kanellopoulos, The Application of the Cluster Model to Nuclear Physics, CERN Report 59-23 (1959).
5 G. C. Morrison, Phys. Rev. Letters 5, 565 (1960).
6 Th. Kanellopoulos and K. Wildermuth, Nucl. Phys. 14, 349 (1960).
7 For the alpha particle cluster in Li^{6} and the Be^{8} cluster in Be^{10} or C^{10}, a harmonic oscillator well consistent with C^{12} rms radius = 2.40 fermis was used.
8 I. Unna, Nucl.Phys. 8, 468 (1958).
9 R. Thieberger, Nucl. Phys. 2, 533 (1956/57).

7. The Decay Scheme of C^{10}

The investigation of the C^{10} decay scheme with the uniform-field beta-ray spectrometer has been delayed by the construction program discussed in Section 2 above. This work will continue about June, 1961. (J. B. Gerhart and G. Sidhu)

II. SCATTERING OF ALPHA PARTICLES AND ALPHA-GAMMA ANGULAR CORRELATIONS

8. Alpha-Particle Scattering by Nuclei in the 2s-1d Shell

The availability of solid state detectors which are thick enough to stop 40-Mev alpha-particles and whose energy resolution approaches 0.6 per cent greatly increases the possible scope of the alpha-particle scattering program. The enhanced resolution allows more accurate determinations of previously measured cross-sections and makes feasible the study of many nuclei, particularly those with odd A, whose level spacings are smaller than the resolving power of scintillation counters. The principal theoretical motivation for continued experiments of this type has been the applicability of the inelastic diffraction scattering model.[1] Analysis of previous experiments[2] have led to the identification of states of collective surface excitation as well as quantitative estimates of the collective surface deformation parameters and strong interaction radii. Nuclei in the 2s-1d shell appear particularly appropriate for study. Many of the low-lying levels should be clearly resolved with the present equipment. Furthermore, previous inelastic scattering experiments,[3,4] in addition to many experiments of different nature,[5] have suggested some substantial success of the Nilsson strong coupling model in this region.

A preliminary study of scattering from Al^{27} is given in this report, and it is hoped that scattering from other isotopes can be examined in the near future. A typical energy spectrum of the alpha-particles scattered by Al^{27} is shown in Fig. 8-1. The state with Q = -2.208 and the doublet at Q = -2.99 Mev are excited more strongly than those with Q = -0.84 (I = 1/2+), Q = -1.013 (I = 3/2+), Q = -2.73 Mev (I = 5/2+) and higher excitations. The angular distributions of alpha-particles leaving the nucleus in the Q = 0, A = -2.208 and Q = -2.99 Mev states are plotted in Fig. 8-2. The oscillations in the excited state angular distributions are out of phase with those of the elastic scattering distribution, and thus indicate, according to the predictions of the inelastic diffraction scattering model, that the state with Q = -2.208 Mev and the contributing member of the Q = -2.99 Mev doublet have even parity. Furthermore, diffraction scattering analysis of the elastic angular distribution gives a value of R_o = 6.19 f for the interaction radius of Al^{27}. This may be compared with the value[3] R_o = 5.97 f for Mg^{24}.

In analogy with previous work[3] on Mg^{24}, a "universal curve" ($\frac{d\sigma}{d\Omega} / k^2 R_o^4$ vs. $2kR_o \sin\theta/2$) is plotted in Fig. 8-3 for the elastic Al^{27} scattering together with Fraunhofer formula. Reasonable agreement is obtained in the range of forward angles between 15° and 35° (corresponding to $X = 2kR_o \sin\theta/2$ between about 4 and 10). The enhancement of the experimental cross-section at small angles is due to Coulomb scattering. The analogous curve for Mg^{24} is also plotted in the same figure and shows fair agreement with the Al data.

The observed inelastic scattering cross-sections indicate that the collective strong coupling model is not appropriate to Al^{27}: (a) According to this model, the level at Q = -2.2 Mev is interpreted to be the second member of the ground state rotational band (I = 7/2, K = 5/2). Analysis of the corresponding inelastic scattering cross-section leads to a value βR_o = 0.89 f. This value is

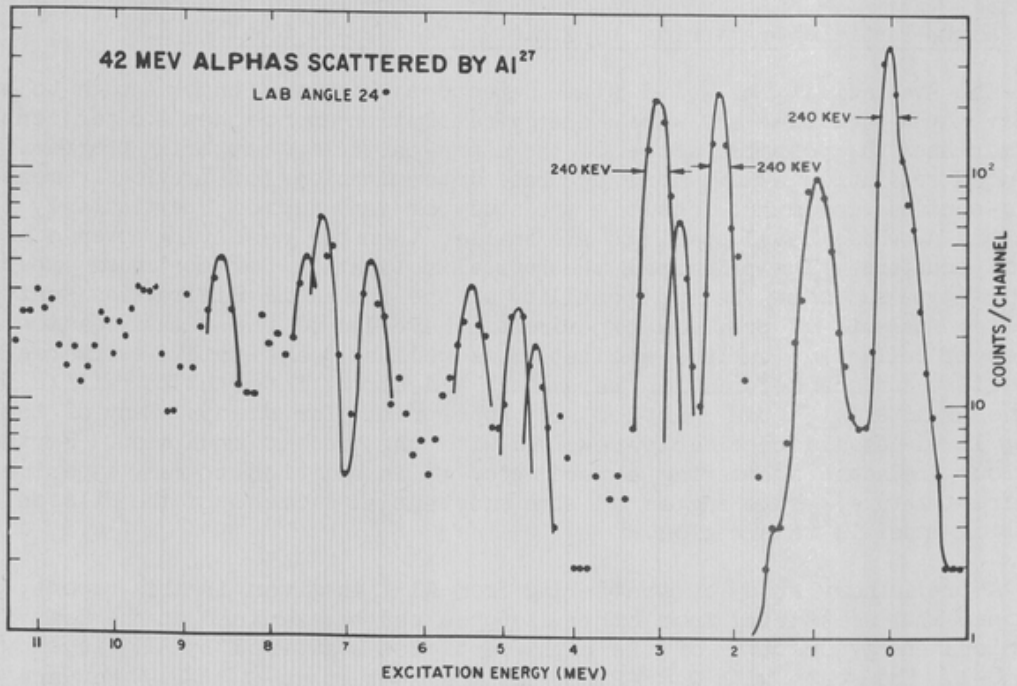

Figure 8-1

Typical energy spectrum of 42-Mev alphas scattered by Al^{27} as detected by a solid state detector. Lab scattering angle is 24°. The asymmetrical shape of the elastic peak is due to particles reaching the end of the depletion region.

distinctly smaller than those obtained for Mg^{24} ($\beta R_o = 1.43$) and other light nuclei with presumed permanent deformations.[6] (b) In the strong coupling description, the other strongly excited level should be the third member of the ground state band ($I = 9/2$, $K = 5/2$). It is difficult, however, to identify such a rotational level with the contributing member of the 2.99 Mev doublet. The location of this state is far too low to conform to a rotational band sequence. Further, the ratio of the cross-sections to the second and third levels is predicted to be (20/7) while the observed ratio is essentially unity.

The inelastic scattering cross-sections are qualitatively consistent with a weak coupling interaction but the cross-sections leading to the less strongly excited levels must be examined before this possibility can be tested critically. (I. M. Naqib)

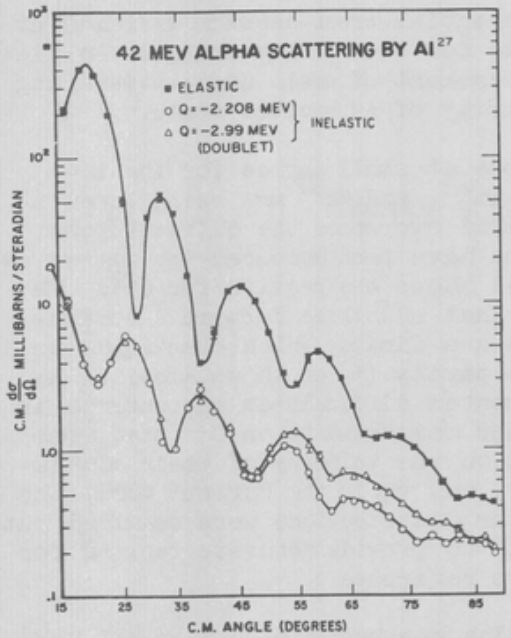

Figure 8-2

Angular distribution of alpha particles leaving the Al^{27} nucleus in the Q = 0, Q = - 2.208, and Q = - 2.99 Mev doublet states.

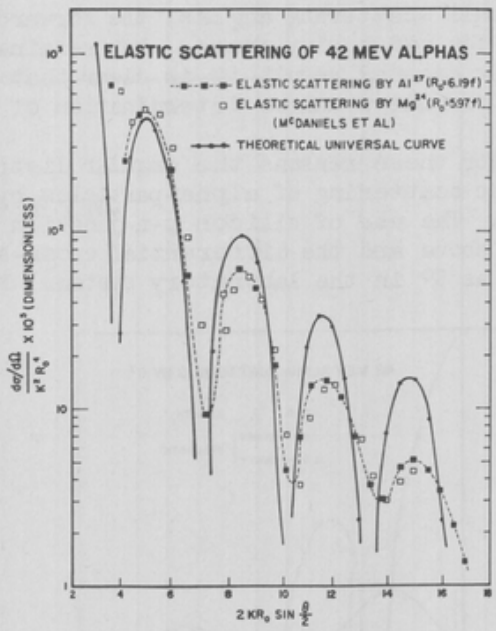

Figure 8-3

Comparison between the elastic scattering by Al^{27} and Mg^{24}, and the Fraunhofer formula.

1 J. S. Blair, Phys. Rev. 115, 928 (1959). E. V. Inopin, JETP 31, 901 (1956), Translation: Soviet Physics JETP 4, 764 (1957). S. I. Drosdov, JETP 28, 734 (1955). Translation: Soviet Physics JETP 1, 741, 788 (1955).
2 McDaniels, et al., Nuclear Phys. 17, 614 (1960).
3 Blair, Farwell, and McDaniels, Nuclear Phys. 17, 641 (1960).
4 A. G. Blair and E. W. Hamburger, Phys. Rev. 122, 566 (1961).
5 H. E. Gove, Proc. Int. Conf. Nuclear Structure, Kingston, 438 (1960).
6 J. S. Blair, Proc. Int. Conf. Nuclear Structure, Kingston, 824 (1960).

9. Inelastic Alpha-Particle Scattering at Small Angles

Previous measurements of the angular distributions of scattered alpha-particles have been limited to laboratory angles greater than about 15° because of poor resolution and the actual physical size of the detectors. However, scattering at small angles is of particular interest, for it is in this region that the simple direct interaction theories are most valid. For example, the Blair diffraction theory[1] involves a calculation based on the Fraunhofer approximation which, as is well known, applies strictly at small angles. It has also been suggested recently[2] that for reasonably small momentum transfers, that is,

for small scattering angles, the forward differential cross-section vanishes at $\theta = 0$ for odd parity change, but remains finite for even parity change. In view of this general result it is clear that a measurement of small angle scattering would provide a unique determination of the parity of an excited state.

For these reasons the angular distributions at small angles for the inelastic scattering of alpha-particles by C^{12}, Ti^{48}, and Zn^{64} are being investigated. The use of silicon p-n junction detectors overcomes the difficulties noted above and the differential cross-sections have been measured for angles as small as 5° in the laboratory system. Fig. 9-1 shows the results for C^{12}. We note that all three forward distributions are finite, which checks the well known parity (+) of these states. Experimental difficulties encountered in earlier measurements on C^{12} cast some doubt on the validity of their conclusions, and so, in the current work, the angular distributions were measured out to 50° to provide accurate results for future reference.

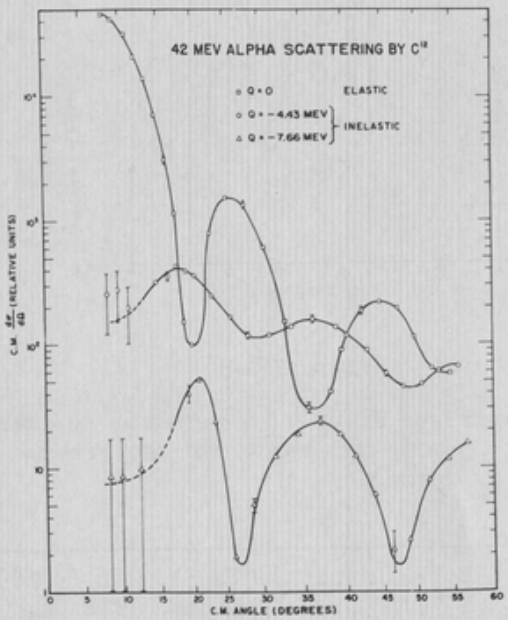

Figure 9-1

Angular distributions for elastic and inelastic scattering of 42-Mev alpha-particles by C^{12}. Experimental errors are shown for only a few representative points.

The measurements on Ti^{48} and Zn^{64} are in progress with emphasis on the anomalous 3- level.[3] In order to establish firmly which final state levels are strongly excited by the inelastic alpha-particle scattering, the heavy-particle magnetic spectrometer has been used to measure precisely the energy spectrum. Fig. 9-2 is a typical spectrum for Zn. We notice in particular the strong excitation of the 3- level at about 3.0 Mev in contrast to the levels between 1 and 3 Mev. The resolution is about 0.30%, and is sufficient to resolve the levels up to about 5 Mev excitation. (D. K. McDaniels, I. M. Naqib, and F. Perry)

1 J. S. Blair, Phys. Rev. 115, 928 (1959).
2 A. J. Kromminga and I. E. McCarthy, Phys. Rev. Letters 6, 62 (1961).
3 G. W. Farwell, D. K. McDaniels, J. S. Blair, S. W. Chen, Nucl. Phys. 17, 614 (1960).

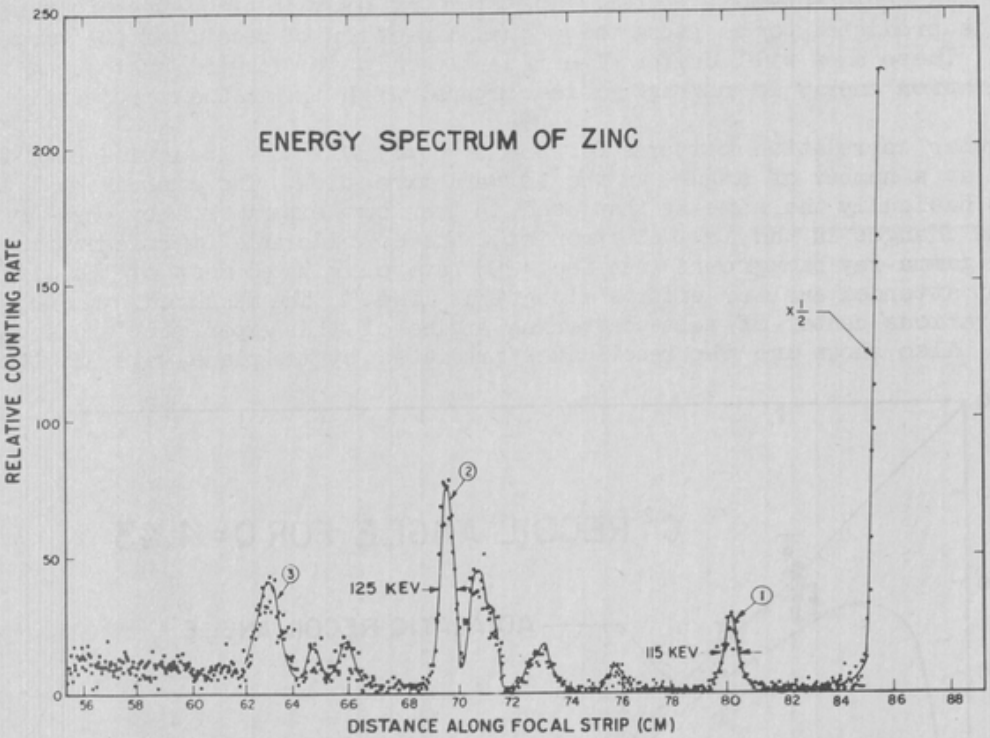

Figure 9-2

Energy spectrum of 42-Mev alpha-particles inelastically scattered from a target of natural zinc. The actual line width is about 120 kev for the clearly resolved peaks labeled (1) and (2), which correspond to excited states at about 1.0 and 3.0 Mev respectively. The latter state is the 3- collective level reported earlier in Zn^{64}. Note the strong, broad level (3) which may also be due to collective excitation.

10. Behavior of the Symmetry Axis in Alpha-Gamma Correlations

By measuring the correlation between the alpha-particle inelastically scattered from the 4.43 Mev level of C^{12} and the de-excitation gamma-ray for a number of scattering angles one can study the behavior of the correlation symmetry axis. The simple Born-approximation theories predict that the appropriate symmetry axis is along the direction of the nuclear recoil.[1] It has recently been pointed out that similar gamma-ray correlation patterns follow directly from the less sweeping assumption that the inelastic scattering amplitude may be calculated in the adiabatic approximation for the relevant nuclear coordinates.[2] There is one significant difference between the adiabatic theory and the plane wave predictions: For the adiabatic theory the symmetry axis for both elastic and inelastic scattering

lies along the direction of recoil for elastic scattering, that is, the symmetry axis makes an angle of $\pi/2 - \theta/2$ with the incident beam, where θ is the scattering angle in the center-of-mass system. The symmetry axis in plane-wave Born approximation is predicted to be along the actual direction of recoil of the target nucleus. These axes will differ significantly only for forward scattering when the excitation energy is nonnegligible compared with the initial projectile energy.

Angular correlation patterns for the C^{12} (α, $\alpha'\gamma$) C^{12*} reaction have been measured at a number of angles in the forward direction. The experimental technique is basically the same as that used in previous experiments by Chen[3] on zinc, with some changes in the fast electronics. The considerable improvement in neutron and gamma-ray background (see Sec. 29) have eliminated most of the difficulties that attended earlier efforts along this line.[4] The measured symmetry angles for the various center-of-mass scattering angles of this experiment are shown in Fig. 10. Also shown are the recoil axes predicted by the plane-wave and the

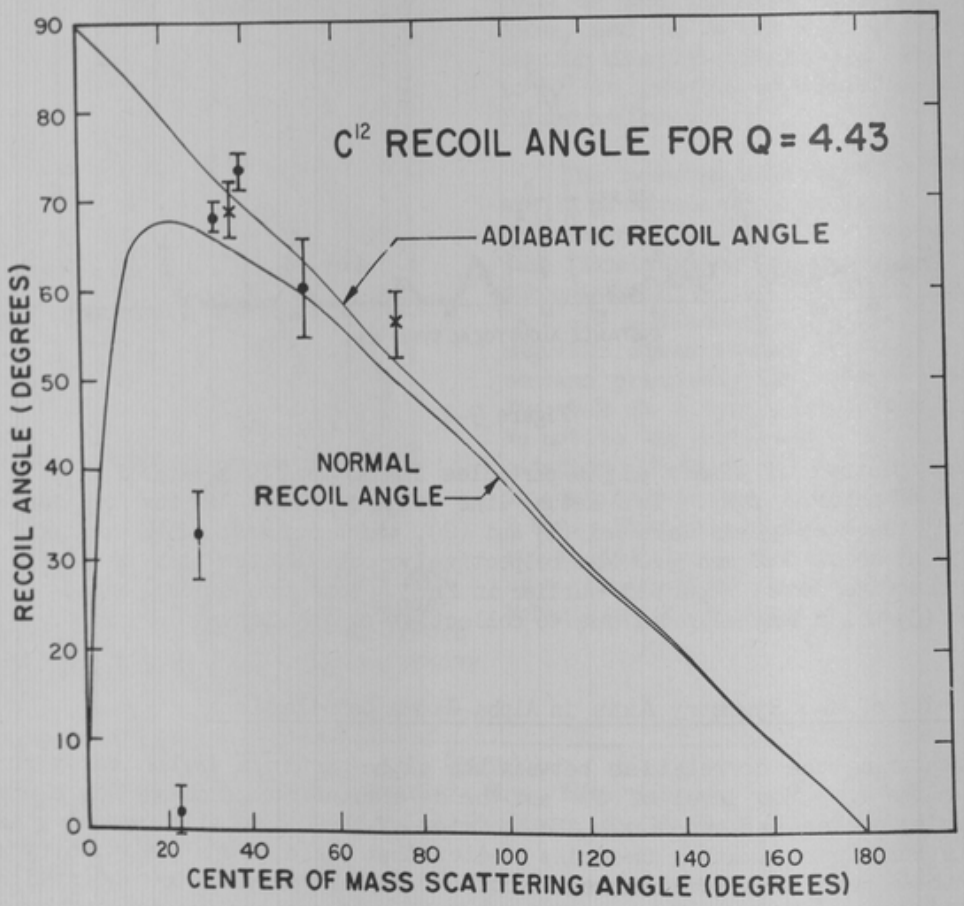

Figure 10

Graph of the symmetry angle, θ_o, versus center-of-mass scattering angle, θ, for excitation of the 4.43 level of C^{12} with 42-Mev alpha particles. The solid curves present the predictions of the plane-wave Born approximation and the adiabatic theory.

adiabatic theories. We note at once the significant deviation from both predictions at forward angles. In fact, the behavior at 24° approaches that expected from a compound nucleus. Further experimental work will be done soon to establish these results more firmly. (W. Brandenberg, D. Hendrie, and D. K. McDaniels).

1 G. R. Satchler, Proc. Phys. Soc. (London) A68, 1037 (1955).
2 J. S. Blair and L. Wilets, Phys. Rev. 121, 1443 (1961).
3 Cyclotron Research, University of Washington (1960), p. 11.
4 G. B. Shook, Phys. Rev. 114, 310(1959).

III. NUCLEAR FISSION

11. The Height of the Fission Barrier and Its Relation to the Level Density

In an earlier report[1] fission excitation functions were given for Bi^{209}, Pb^{208}, Pb^{207}, Pb^{206} and Au^{197}. From these functions fission barrier heights B_f were estimated for the compound nuclei involved by means of the simple theoretical expression

$$\Gamma_f/\Gamma_n = C' \exp 2\left[\sqrt{a_f (E - B_f)} - \sqrt{a_n (E - B_n)}\right].$$

Here Γ_f is the average fission width and Γ_n is the average width for neutron emission in the compound nucleus. E is the excitation energy and B_n is the binding energy of a neutron in that nucleus. a_n and a_f are the parameters that appear in the expressions of the form

$$W = C \exp 2\sqrt{aE}$$

for the level density in the Fermi gas model; a_n refers to the daughter nucleus that appears following neutron emission, while a_f pertains to the distribution of levels in the fissioning nucleus at the saddle-point of the fission process. For a Fermi gas at constant density, the parameter a is proportional to the number of particles. Therefore, if the system, apart from the emitted neutron, is regarded as a Fermi gas of constant density, we would expect that a_f and a_n should be almost identical. However, in order to fit the measured excitation functions to the first equation, it is necessary to take a_n significantly smaller than a_f. This discrepancy can be explained: In these experiments the nuclei in question are near magic, and at low excitation energies the level densities are consequently smaller than for a Fermi gas, and a_n is smaller than what we will describe as the normal value a_o for nuclei in the general neighborhood. On the other hand, a_f refers to the nucleus in a highly distorted condition in which the strong binding effect of the closed or almost closed shells has been lost, and we would anticipate that the Fermi gas model provides a more satisfactory description and that a_f should be close to a_o.

In the course of further considerations, there were brought out two points of interest in connection with the distribution of levels: We will write, in the form of an earlier equation, an expression for the density of levels in a near magic nucleus:

$$W_n = C \exp 2\sqrt{a_n E}.$$

However, we will now understand that a_n is not necessarily a constant, but is itself a function of E. Our first point of discussion is concerned with this functional relationship. The results given in the preceding paragraphs show that a_n is small at low excitation, and rises to the normal value at higher excitation where the effect of the outer closed shell has disappeared. But in this perturbation the individual levels are preserved. The effect of the magic character is to depress the ground state by an amount E_{dg} and to depress the higher states by amounts E_d that become generally smaller for larger values of the excitation energy E. We would not expect a simple relation between E_d and E, but we will

make the reasonable assumption that the average depression for a group of neighboring levels can be represented by a simple decreasing function approaching zero asymptotically, and, to be specific, we shall write

$$E_d = E_{dg} \exp(-E/E_r)$$

wherein E_r is a parameter that provides a measure of the excitation required to rise above the magic character of the nucleus. Now it follows that the relation connecting E and a_n is

$$\sqrt{a_n} = \sqrt{a_o}\sqrt{1 - (E_{dg}/E)\left[1 - \exp(-E/E_r)\right]} + \\ + (1/\sqrt{E}) \log \sqrt{1 - (E_{dg}/E_r)\exp(-E/E_r)}$$

We will consider the interpretation of the fission reaction $Bi^{209}(\alpha, f)$ in terms of these relations. For the compound nucleus At^{213}, E_{dg} = 5 Mev.[2] From its definition, $E_r > E_{dg}$; it seems unreasonable that E_r could appreciably exceed 20 Mev. Accordingly, curves based on the equation above were constructed giving a_n/a_o as a function of E for the quoted value of E_{dg} and for E_r = 5, 10, and 20 Mev; these are shown in Fig. 11. For the values of E corresponding to

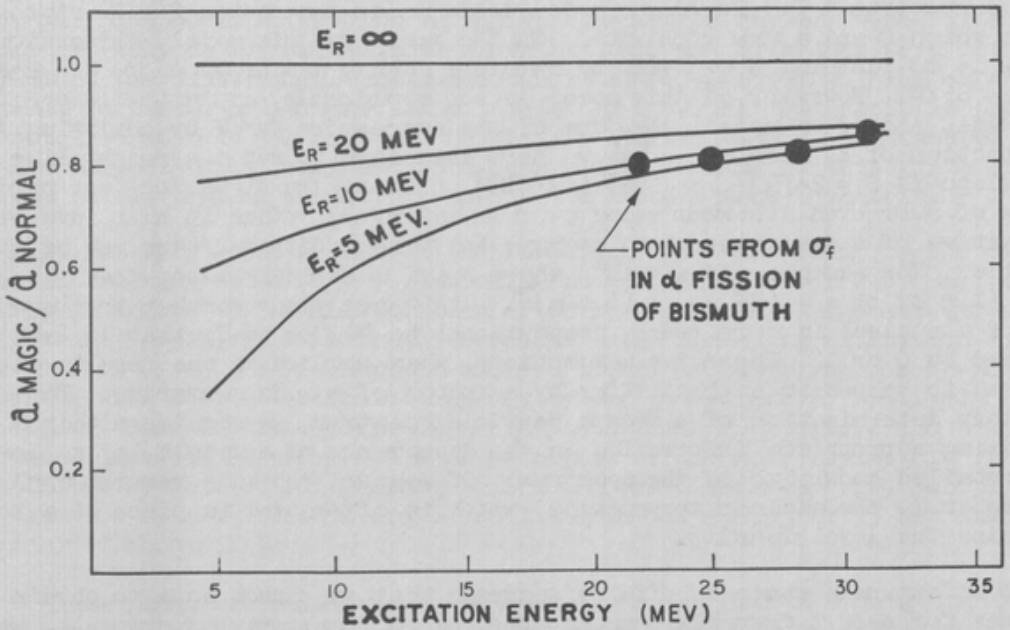

Figure 11

The energy dependence of the function a_n in a near-magic nucleus where the ground state is depressed 5 Mev by shell effects.

this experiment, the ratio has values close to 0.8. Values of a_n/a_f, which, according to our discussion is essentially the same as a_n/a_o, were obtained from the analysis of the fission excitation function, and are plotted on the same graph. It is gratifying to find the empirical results in good agreement with the calculations. Unfortunately, it is not possible to determine from these results the value of E_r.

The problem of evaluating E_r is an interesting one. It is similar to the question of the recovery from depression of energy levels by pairing of nucleons in even-even nuclei. It has been generally assumed that with excitation equal to neutron binding energies ($\sim$8 Mev) the depression associated with pairing has virtually vanished.[3] Information on the corresponding disappearance of the effect of complete shells should be revealed by an examination of the spectrum of emitted neutrons for an excitation of the residual nucleus between 5 and 10 Mev. In this range the ratio a_n/a_o is more sensitive to E_r than at the higher energies of the present experiment. Some data of this sort are already available.[4] As one would expect, they lead to values of the ratio lower than those obtained from fission experiments, and indicate, therefore, values of a_n considerably smaller than the value of a for a Fermi gas. As yet, the analysis is too ambiguous to provide reliable estimates of E_r.

This brings us to the second point for discussion: the difficulties that are encountered in the attempt to determine the value of a from a measurement of a particle spectrum. The Fermi gas model leads to an expression for W written above, in which C and a are constants. On the basis of this model, the obvious procedure is to plot log W vs. $\sqrt{E}$, to obtain a straight line of slope $S = 2\sqrt{a}$, whence $a = S^2/4$. However, if this model is not applicable, as in the case of near magic nuclei, and if we retain the form of the expression for W by admitting that a is a function of E, then the graph we have described is not a straight line, and its slope is $S = 2\sqrt{a}\left[1 + (E/a)\,(da/dE)\right]$. Thus, the slope does not provide a measure of a or even its mean value over an interval; rather it also involves the derivative of a with respect to energy, and this additional term may be quite appreciable. For example, if $a = AE^m$, where A and m are constants, then $S = 2\sqrt{a}\,(1 + m)$ or $a = (S^2/4) / (1 + m)^2$. It is not clear whether the level density of a nucleus is more nearly proportional to $\sqrt{E}$ or to E; that is, whether m is nearer to 0 or 1. These two assumptions, when applied to the results stated above, lead to values of a that differ by a factor of 4. To summarize: To make a satisfactory determination of a from a particle spectrum, we require either a theory giving appropriate information on the dependence of a upon E, or an unusually detailed knowledge of the spectrum. Of course, the same remarks apply to the parameter T, the nuclear temperature, which is often used in place of a to characterize the level density.

This unfortunate state of affairs suggests that we cannot hope to obtain good values for a or T from the spectra observed in low energy experiments, where we expect these parameters to depend sensitively upon E. The variation of a or T with E is less pronounced at higher energies, but under these conditions, other difficulties appear: The spectra from high energy bombardments are usually superpositions of a variety of spectra corresponding to a sequence of evaporations, and it is difficult to disentangle the separate components. In spite of these difficulties the values of these parameters are sufficiently fundamental to make this problem a very interesting one. Perhaps some of the uncertainties that have

beclouded this field of investigation will disappear as more data are accumulated, especially data that will indicate the variation of these parameters with energy. (I. Halpern and W. J. Nicholson, Jr.)

---

1 Cyclotron Research, University of Washington (1960), p. 10.
2 A. G. W. Cameron, Chalk River Report CRP-690 (1957).
3 H. Hurwitz and H. A. Bethe, Phys. Rev. 81, 898 (1951).
4 K. J. LeCouteur and D. W. Lang, Nuc. Phys. 13, 32 (1959). Recent measurements by D. B. Thomson and L. Cranberg (private communication).

---

12. Angular Distributions of Selected Fission Fragments From 43-Mev Alpha-Particle Bombardment of Lead

The apparatus shown in Fig. 12-1 (12-1a, 12-1b) has been used to measure the angular distributions of fission fragments emitted in the bombardment of natural lead and thorium targets with 43-Mev alpha-particles. The angular resolution of about 18° is fairly large, but was necessary in order to obtain sufficient intensities. Fragments which passed through the slots of the assembly were stopped in aluminum foil placed around the outside of the semi-cylinder. The foil covering each slot was processed radiochemically for specific fission fragments, and the relative cross-section for the production of each fission product was plotted as a function of angle. Parametric curves[1] were fitted to the experimentally determined angular distributions, and from them were determined values of the differential cross-section ratio $\sigma(0^{\circ})/\sigma(90^{\circ})$. The experimental results for natural lead are shown in Fig. 12-2, where that ratio is plotted versus the ratio of the mass of the fission fragment which was measured to that of its complementary fragment. The interesting feature of this graph is the increase in the angular anisotropy as fission becomes more symmetric.

We interpret this result in the following way: According to the theory of fission fragment anisotropy[1], fissioning nuclei of high spin but small excitation energy in excess of the fission barrier energy have very large anisotropies. For a given high spin the anisotropy decreases with increasing excitation energy. In the present case, the Po compound nucleus formed on capturing the 43-Mev alpha-particle will have an excitation energy around 35 Mev and a relatively large average spin. Some of these compound nuclei will fission promptly, and with a symmetrical mass distribution. The anisotropies of the more asymmetric fragments (described by mass ratios greater than 1.23) are consistent with our picture of the fission of a species having a total excitation energy of 35 Mev and a fission barrier of about 20 Mev.

Those compound nuclei which emit a neutron instead of undergoing fission are left with about 27 Mev of excitation energy and still have high average spins, since the emitted neutron carries off relatively little angular momentum. Some of these nuclei will undergo "second chance" fission, and their much lower excitation energy implies a much larger angular anisotropy for these fission fragments. We attribute the increase in anisotropy of fragments of mass ratio less than 1.23 to an admixture of highly anisotropic second chance fissions with the less anisotropic first chance fissions, the relative proportions being governed by the mass-yield distributions and the probabilities of first- and second-chance

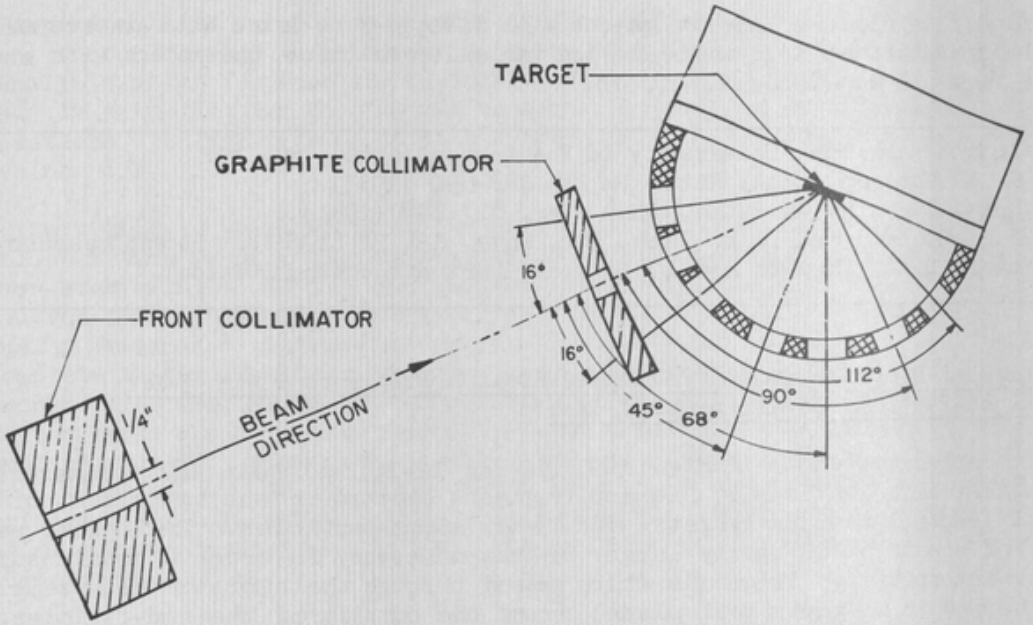

Figure 12-1(a)

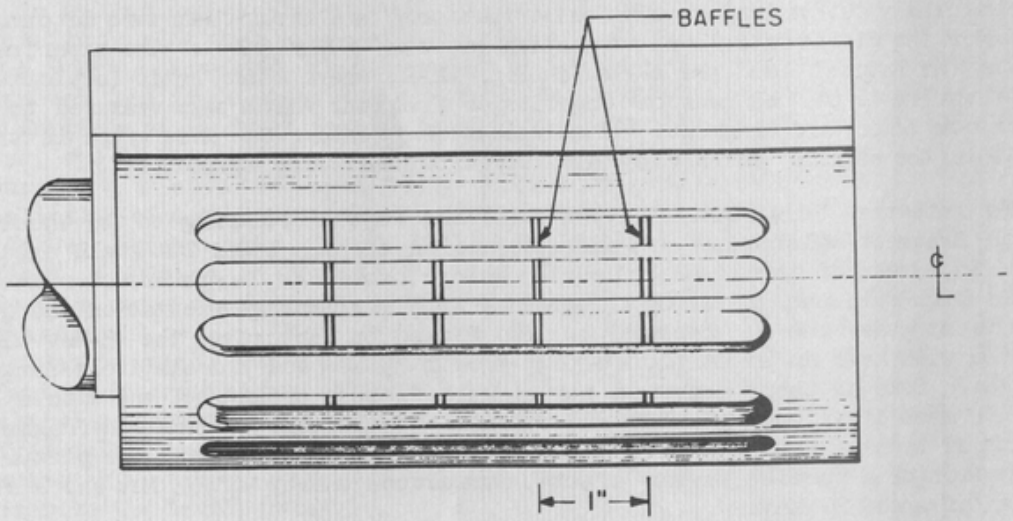

Figure 12-1(b)

Figure 12-1

Apparatus for measuring the angular distributions of fission products from lead and thorium targets bombarded with 43-Mev alpha-particles. One view shows the plan of the apparatus; the other view shows the details of the semi-cylinder.

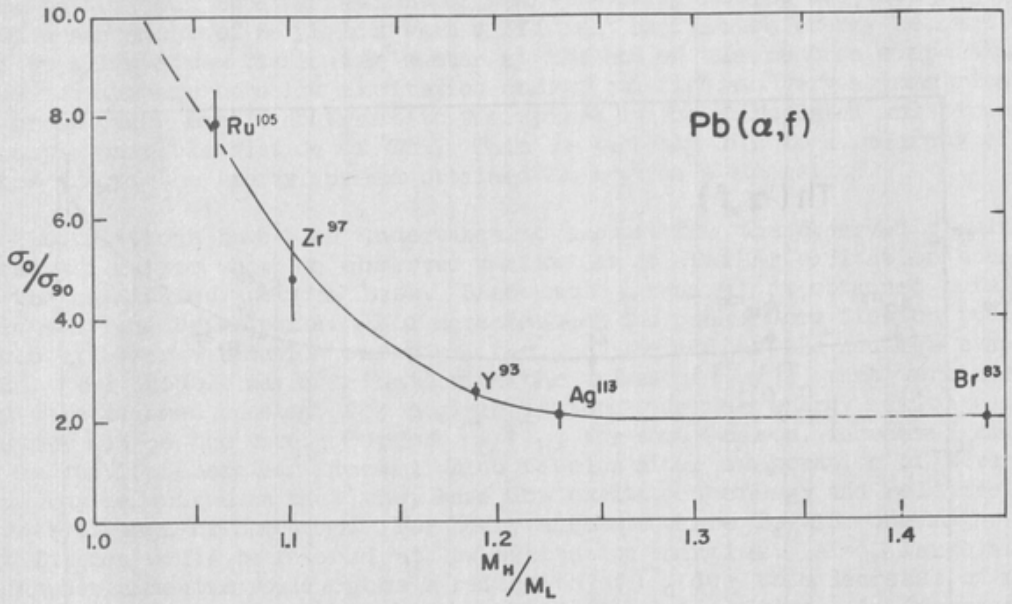

Figure 12-2

Anisotropy of fission fragments from 43-Mev alpha-particle bombardment of natural lead plotted as a function of the mass ratio of the fission fragment pair.

fission. The data of Fig. 12-2 imply that the mass distribution curve of second chance fission is very much narrower than that of first chance fission. The experimental results can be reproduced by a combination of two simple mass distributions: One includes 80 per cent of the fissions, and is a broad symmetric distribution representing first chance fission from a species having a fission barrier of 20 Mev. The remaining 20 per cent of the fissions have a distribution which is symmetric and very narrow, the full-width at half-maximum being only 10 mass units wide; this is attributed to the second chance fission of a species with a fission barrier of around 22 Mev. Further work is in progress to check this conclusion experimentally, by bombarding Pb^{207} with lower energy alpha-particles and examining the mass distribution curve of the fission fragments.

Fig. 12-3 shows the angular anisotropies of fission fragments from a thorium target bombarded with 43-Mev alpha-particles. The anisotropy fission evidently bears little relation to the asymmetry, except perhaps when the asymmetry becomes very great as in the case of Ge^{77}.

In the heavier elements the fission barriers are very much lower, perhaps as much as 6 Mev, than they are for elements in the region of lead. Consequently anisotropies are much smaller for all fissioning species except the last one. In the present case, theory predicts anisotropies of 1.4, 1.5, and 2.4 for first, second and third chance fission, respectively. The data of Fig. 12-3 imply that

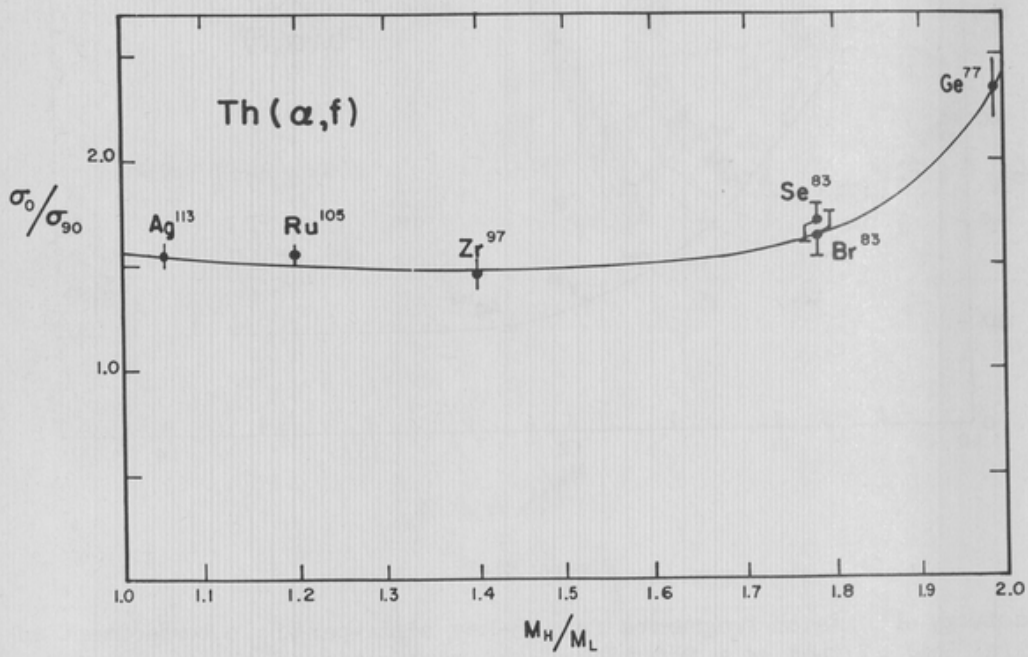

Figure 12-3

Anisotropy of fission fragments from 43-Mev alpha-particle bombardment of thorium plotted as a function of the mass ratio of the fission fragment pair.

most of the fission products are formed in first and second chance fission. Evidently the low-yield and more anisotropic Ge^{77} comes predominantly from third chance fission. (A. W. Fairhall and R. E. Wilson)

---

1 I. Halpern and V. M. Strutinski, Proceedings of the Second International Congress of Peaceful Uses of Atomic Energy, 15, 410 (1958).

---

13. Peak-to-Valley Ratios for Alpha-Particle Induced Fission of Thorium

Radiochemically determined Ba^{139}/Ag^{113} ratios at small forward angles for alpha-particle induced fission of Th were given in an earlier report.[1] A broad peaking of these ratios with a maximum of 7 to 8 was observed for about 27-Mev

incident alpha-particles. Another small rise has been observed for about 35-Mev alpha-particles. Such variations of peak-to-valley ratios are thought to be due to an enhancement of Ba yields when sufficient excitation energy becomes available to allow a new fissioning member at the end of the neutron evaporation chain. These new members have low excitation energy and fission very asymmetrically. The broad peaks are in contrast to the spikes in the calculated anisotropies of the alpha-particle fission of Th^2. This is probably due to a smearing of the spikes due to the energy spread obtained in neutron evaporation.

Calculations have been undertaken to account for the observed results. The calculated ratios show the observed variations at similar excitation energies but the magnitudes are much less. Reasonable agreement is obtained outside the regions of the broad peaks. For agreement at the peaks more fission would be required at lower excitation energies, i.e., at the end of the neutron evaporation chain. The trouble may originate with the values of Γ_f/Γ_n that were used. They were assumed constant for a given isotope over the energy region considered. This may not be the case. Suppose Γ_f/Γ_n, for some reason, increased sharply at low excitation energies. Nuclei which fission after evaporation of several neutrons may be unique in that they have low excitation energy and relatively large amounts of angular momentum. For heavy elements where $B_f < B_n$ one might expect that fission would be favored at low excitation energies. Also, large amounts of angular momentum would cause a reduction of Γ_n due to a decrease of normal excitation energies, and thus a decrease in level densities. An increase in Γ_f/Γ_n at low energies is being investigated in an attempt to account for the observed variations of the peak-to-valley ratio. (J. A. Coleman and A. W. Fairhall)

---

1 Cyclotron Research, University of Washington (1960), p. 14.
2 I. Halpern and V. M. Strutinski, Paper P/1513, Second U. N. Conference on the Peaceful Uses of Atomic Energy, 1958.

---

14. Alpha-Particles Emitted in Fission

Alpha-particles are sometimes produced in fission, the probability being about 0.003. From the energy of the alpha-particles, and from their angular distribution relative to the paths of the fission fragments, it appears that the alpha-particle emerges from a point between the fragments immediately after their formation.[1] The kinetic energy of the alpha-particle can be attributed almost entirely to the electric repulsion of the fission fragments. And so it appears that the alpha-particles are produced with very little kinetic energy. In the language of the liquid drop model, these alpha-particles have been called droplets which are left behind during the division of the system into the two large drops. In the course of discussions with R. Nobles and R. B. Leachman regarding their work on the frequency of alpha-particle emission in fission,[2] it became clear that the formation of these droplets must entail rather unusual and violent interactions. An alpha-particle within one of the fragments which is in its ground state has a binding energy which may be quite negligible. But a free alpha-particle between the fragments must have a potential energy which is about

20 Mev more than that of the bound alpha-particle. This energy corresponds to the height of the Coulomb barrier for an alpha-particle. The problem is to understand how a nuclear alpha-particle can acquire this much energy in the short time available during scission. An adiabatic process would deliver to an alpha-particle a small share of any available excitation energy--a quantity corresponding to the nuclear temperature. The probability that an alpha-particle would receive 20 Mev is negligible. Presumably scission is highly non-adiabatic (see Sec. 16). We conceive of a violent snapping or tearing of the neck at scission. The fragments presumably snap back from a stretched to a spherical shape very suddenly, and the interaction of an alpha-particle with the nuclear walls accomplishes a large transfer of energy in a short time.

A calculation to determine whether such a mechanism could conceivably account for the observed yield of alpha-particles was made with the following model: An alpha-particle is initially in a state of low kinetic energy in a one-dimensional square well. Suddenly a square barrier appears in the center of the well. Using the sudden approximation[3] we can find the probability that the alpha-particle will be found in the region of the barrier, that is, between fragments, with an energy above the height of the barrier (see Fig. 14). With reasonable values for the energies and dimensions involved, an estimate of this sort leads to a probability of $\sim$ 5 per cent for the production of a free alpha-particle in the central region. If we include a factor for the probability that four suitable nucleons are clustered into an alpha-particle in the original nucleus, and a factor to account for the finite time required for fission snap-off, then the estimated probability is reduced. But it would seem that the observed probability remains within reach of this model. Further work with the model is in progress. It is interesting to note that a very similar model has recently been applied to neutron ejection in fission.[4] (I. Halpern)

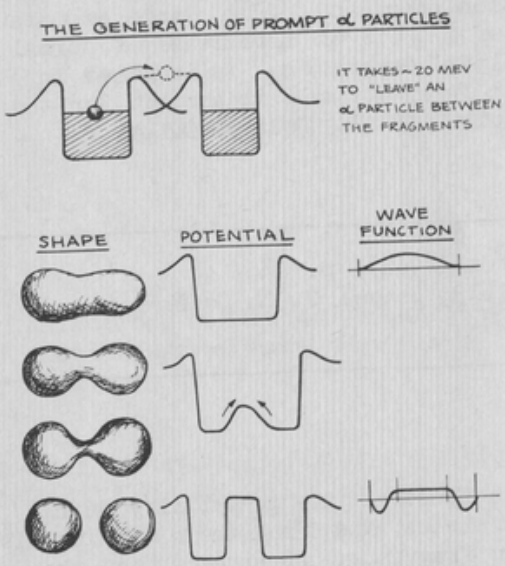

Figure 14

Model used to estimate α production in fission by non-adiabatic snapping apart of fragments.

1 See for example N. A. Perfilov in "Physics of Nuclear Fission," Supplement to Atomnaya Energ., Pergamon, New York, 1958.

2 R. Nobles and R. B. Leachman, "Measurements of α/f ratios in Spontaneous Fission," (private communication).

3 L. I. Schiff, "Quantum Mechanics," McGraw-Hill Co.

4 V. S. Stavinsky, JETP (36) 437 (1959); R. W. Fuller, "Non-Adiabatic Changes of Potential and Neutron Production in Fission," Ph.D. thesis, Princeton University.

15. Ternary Fission

An investigation has been initiated of the production of alpha-particles by the fission of moderately excited nuclei. Of prime interest is a correlation of the abundance, angular distribution, and energies of these alpha-particles with respect to those of the coincident fission fragments. Several large area n-i-p solid state detectors were fabricated for use as fission fragment counters. These counters failed after about two months due to breakdown of the junctions. Presently, a large area surface-barrier solid state detector is used to count fission fragments and a plastic scintillator is used as the alpha-particle counter. A second solid state detector will subsequently be inserted as an opposing fission fragment counter. A fast and a slow pulse are taken from each counter. The fast pulses are fed into a fast coincidence circuit[1] with a resolving time shorter than the time between successive beam bursts from the cyclotron. This system has reduced the number of accidental coincidences to an acceptable level. The coincidence output is used to gate the slow pulses which are then each displayed on a multichannel analyzer.

To date only the 42.5-Mev alpha-particle induced fission of U^{238} has been studied. Although the small amount of data taken is promising, one cannot yet state that alpha-particles have definitely been observed in coincidence with fission. Future experiments are planned which will establish the role of accidentals which, at the present time, may be masking the true fission alpha-particles. (J. A. Coleman, D. Drake, A. W. Fairhall, and I. Halpern)

---

1 Cyclotron Research, University of Washington (1960), p. 43.

---

16. The Angular Correlations of the Neutrons Emitted in Fission and Their Relation to the Torques Acting at Scission

That stage in the fission process where the two fragments separate so that they are no longer under the influence of each other's nuclear forces is called scission. There are reasons for believing that this separation is violent and non-adiabatic. For example, it is argued in Sec. 14 that for alpha particles to be emitted during fission, as they sometimes are, it is necessary that the nuclear shape at scission change very rapidly.

We can picture scission as a quick tearing of the thin neck of nuclear matter matter joining the fragments. If such a tearing is sufficiently chaotic and disorganized, it may give rise to sizeable torques between the fission fragments. We can make a very rough estimate of the amount of angular momentum likely to be imparted to each of the fragments by such torques. We assume that the tearing is so haphazard, that the probabilities of various internal states of the new fragments are governed only by a Boltzmann factor. If the tearing is subject to constraints which compel it into some regular course, this assumption is not valid, but to the extent that the tearing is truly random, the assumption is justified. Then a typical fragment will receive an angular momentum, J, such that

$$\frac{J^2\hbar^2}{2\mathcal{I}} = kT$$

where T is the "temperature" appearing in the Boltzmann factor. The use of T does not imply the assumption of thermal equilibrium. Rather, T should be regarded as a parameter that provides a coarse description of the distribution of nucleon energy levels. If there happen to be no restrictions on the availability of nucleon states, then the value of T should be close to the normal value for a nuclear temperature. At the time of their formation, the fragments are elongated along the separation direction. The largest moment of inertia of a fragment is one about an axis perpendicular to this direction. Therefore, the component of angular momentum perpendicular to the separation direction will tend to be large compared to the component parallel to it. The rigid body estimate of $\hbar^2/2\mathcal{I}$ for a transverse axis is about 4 kev. Taking kT $\sim$ 1 Mev, we are led to J $\sim$ 15. We will expect each fragment to have an angular momentum, roughly of this order, and we will expect that its direction will tend to be perpendicular to the separation direction.

The introduction of such large amounts of angular momentum at scission was first suggested by Strutinsky[1] to explain the unexpectedly large amount of prompt gamma-radiation in fission and the observed correlations of this radiation with the paths of the fission fragments. Studies of isomers produced in slow neutron fission also provide indications that the fragments have large angular momenta, but here the evidence is still somewhat ambiguous.[2]

It should be possible to learn something about the angular momenta given the fragments at scission through an examination of the angular correlations of fission neutrons. Some methods for studying such correlations are being explored and will be briefly discussed below.

(1) The most direct arrangement would employ two fairly efficient fast neutron detectors to measure the azimuthal correlation of neutrons emitted from a single fragment. (The "mother fragment" can be fairly reliably identified, because the neutrons share its momentum and tend to be emitted into a cone about the fragment direction). If the fragment has a sufficiently large angular momentum, the neutrons should all tend to come off perpendicular to the rotation axis. It might be possible to observe such a tendency by looking for a correlation as a function of azimuthal angle about the fragment direction. If a correlation is found, it would be interesting to move one of the counters to examine neutrons from the other fragment. This might let one learn whether the spins of the two fragments tend to be parallel or not, i.e., it could provide information about the way in which angular momentum is divided between the spins of the individual fragments and the orbital momentum between them.

(2) A less direct method of finding a neutron correlation is to detect a single neutron and both fission fragments. The fragments will not appear in opposite directions, but will show the effects of neutron recoil. If the paths of all emitted neutrons are concentrated in a plane, then the paths of the two fragments will, in general, tend to lie in that plane. This measurement provides less information than the first one, but it has the advantage of requiring only neutron detector.

(3) Finally, it might be possible to demonstrate an effect without detecting even one neutron. The width of the angular correlation function for the two fragments depends upon the correlation of the fission neutrons, and would be affected by the neutron correlation we are discussing. Unfortunately, this effect is small and subject to confusion by scattering of the fragments. There is a slight suggestion of such an effect in higher energy fission,[3] but it is too small to be conclusive.

If some of the prompt neutrons are ejected during scission, as suggested by Fuller[4] and Stavinsky,[5] the interpretation of correlation studies such as those suggested would be complicated. It is also conceivable that the fragments with high angular momenta would have a strong tendency to emit photons rather than to evaporate neutrons, and thus to reduce the effect in question as well as to complicate the interpretation.

Explorations are being carried out on the feasibility of these experiments for estimating the torque acting during scission by studying the angular correlation of the emitted neutrons. (D. Drake and I. Halpern)

---

1 V. M. Strutinsky, JETP 37, 861 (1961).
2 L. Glendenin (private communication).
3 W. J. Nicholson and I. Halpern, Phys. Rev. 116, 175 (1959).
4 R. W. Fuller, "Non-Adiabatic Changes of Potential and Neutron Production in Fission," Ph.D. thesis, Princeton University (1961).
5 V. W. Stavinsky, JETP 36, 437 (1959).

IV. RADIATIVE CAPTURE AND HEAVY FRAGMENT EMISSION

17. A Study of the O^{16} (d, γ) F^{18} Excitation Function

Some previous work at this laboratory included the investigation of the N^{14} (α, γ) F^{18} excitation function.[1] The work described here is the determination of the excitation function for O^{16} (d, γ) F^{18}. A comparison of the two excitation functions should provide a clue as to whether the reactions proceed through a compound nuclear mechanism or some process involving "capture from an orbit." The first mechanism may be expected to lead to similar excitation functions for these two reactions, while the second mechanism should yield distinctly different functions owing to differences in the dipole interactions.

The technique used is the "stacked chamber" technique described in the previous investigation.[1] The target gas is oxygen and the catcher foils are of aluminum. The high induced Na^{24} activity in the foils necessitates a chemical separation to make counting feasible. The technique used was to dissolve the foils in 0.2 N NaOH and get rid of the Na^{24} by running the solution through a Dowex-1 anion exchange column and washing with 0.2 N NaOH. The fluorine remains on the resin and was counted as such by means of the 0.51-Mev annihilation radiation.

Preliminary results using natural oxygen indicate a curiously smooth curve with no strong dependence on energy in the range from 21 to 10 Mev. Further work is continuing with natural oxygen to verify this shape and with isotopically enriched oxygen to determine the contribution of the O^{18} (d, 2n) F^{18} reaction to the total F^{18} activity. (N. E. Erickson[1] and A. W. Fairhall)

---

1 Mr. Erickson is a O.R.I.N.S. Fellow studying in the Department of Chemistry.

---

18. The He^3 (He^4, γ) Be^7 Reaction

Activation of He^3 by He^4 at bombarding energies below 38 Mev has been reinvestigated using specially purified He^3 after it was concluded that the previously-measured[1] cross-sections of the reaction He^3 (He^4, γ)Be^7 were too high owing to activation of a trace of air impurity. The remeasured values are shown in Fig. 18. At bombarding energies greater than 38 Mev the cross-section appears to increase sharply. However, about 1 per cent air in the He^3 target would suffice to account for this effect. Below about 28 Mev bombarding energy activation of impurities cannot account for the observed production of Be^7.

The He^3 (He^4, γ) Be^7 reaction may have important astrophysical implications. The increase in the cross-section at lower bombarding energies suggests that the excited states of Be^7 between 4 and 8 Mev may give rise to resonances in the capture cross-section at these excitation energies of the compound nucleus. A resonance at the 3.0 and 4.6 Mev excited states of Be^7 could lead to the production of large amounts of Be^7 in stellar material which is rich in He^3 and He^4

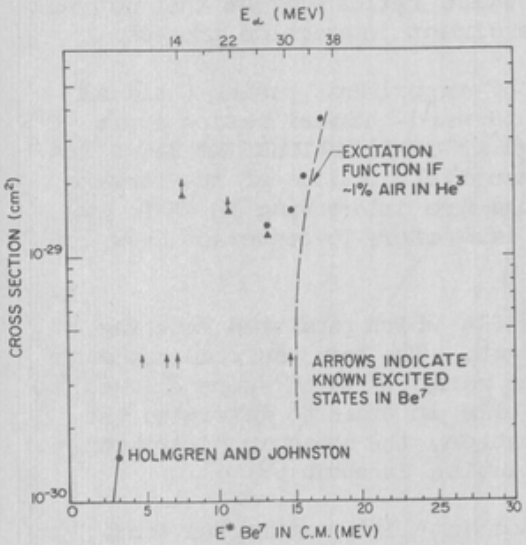

Figure 18

Observed excitation function of the reaction He^3 (He^4,γ) Be^7. The increase in the cross-section above 28 Mev may be due to activation of air impurity in the target.

and which has a large temperature and density. Such conditions presumably exist during the collapse of a star leading to a supernova. This may lend some experimental support to the suggested explanation[2] of the light curve from Type I supernovas as being due to Be^7. Further experiments are planned in an attempt to measure the cross-section of the reaction at lower energies in the region of the excited states of Be^7. (A. W. Fairhall)

---

1 Cyclotron Research, University of Washington (1958), p. 9.
2 L. B. Borst, Phys. Rev. 78, 807 (1950).

---

19. The Emission of Heavy Fragments in Reactions Induced by Helium Ions

In 1959 Bouchard reported[1] observing Be^7 fragments from helium ion bombardment of O and Al. Preliminary angular distribution data of Bouchard indicated that the Be^7 fragments were emitted only in the forward direction with respect to the beam, and some kind of direct interaction process was suggested for the reaction mechanism. Subsequently, work was undertaken to develop an ionization chamber capable of observing other fragments, not amenable to radiochemical investigation, which might also result from helium ion bombardment of light elements. This ionization chamber and some of the measurements made with it were reviewed in last year's progress report.[2]

Richard Lindsay, of Washington State University, repeated Bouchard's angular distribution work and obtained conflicting results.[3] Further checking at this laboratory demonstrated that the reaction mechanism could not be assumed to be a direct interaction, and more detailed radiochemical experiments were indicated. It is these experiments that will be reported here. We feel that it is advantageous to exhaust radiochemical techniques before returning to counter techniques.

The angular distribution work of Bouchard and of Lindsay was really a forward-backward ratio experiment. That is, the Be^7 activity found in a catcher foil in the forward direction with respect to the target was compared with the activity found in a backward catcher foil. If Mg or Al are used as the target, the kinematics of a compound nucleus reaction are such that an appreciable fraction of the Be^7 product should find its way to the backward hemisphere, providing that the target is thin enough. The forward-backward ratios were recently

remeasured for Mg and Al and were found to be about 3.5:1 in both cases. The target thickness was 1.3 mg/cm^2 for Mg and 1.1 mg/cm^2 for Al. These results agree reasonably well with those of Lindsay.[2] These ratios suggest that not all of the Be^7 cross section can be attributed to a direct interaction process.

It was then decided to undertake a series of experiments, using O and Al targets, with these objectives: (1) to obtain forward-backward ratios about 90° in the center of mass system; (2) to obtain angular distributions, at least in the forward hemisphere; (3) to determine momentum distributions of the forward moving Be^7 fragments. The momentum distributions are interesting in their own right, and are also necessary to calculate the laboratory-to-center-of-mass conversion factors.

For these purposes a target assembly was built which permitted mounting catcher foils in 4π geometry around a thin target. The beam was collimated to 1/4 inch diameter. Be^7 fragments emitted in the range 0° to 16° were allowed to bury themselves in a stack of 2.5 mg/cm^2 gold foils in order to determine the range distribution and, by a suitable transformation, the momentum distribution. From geometric considerations, the angular resolution is about 5°.

In order to translate the range distribution data into meaningful terms, it was necessary to know the range-energy relation for Be^7 ions in Au. Published means of estimating the range-energy relation of Be ions proved to be quite divergent, and it was decided to resort to experiment. Helium ions were directed at a thin Be^9 target and the elastically scattered Be^9 ions, after traversing various thicknesses of Au, were detected in a calibrated solid state counter. The corresponding alpha particle was detected in a CsI crystal and a coincidence was demanded between the two counters. The resulting range-difference data was extrapolated to zero Au thickness and converted to a range-energy relation. A mass correction factor was applied to convert from Be^7 to Be^9. Preliminary results are given in Fig. 19-1. The error limits represent the uncertainty in extrapolating the range-difference curve. Further work is planned to reduce these error limits.

Fig. 19-2 presents the energy distribution of Be^7 fragments from helium ion bombardment of Al. Only the forward moving fragments in the angular range 0° to 16° were collected. The vertical line represents the maximum energy that the Be^7 can have from this reaction. Considerable difficulty was experienced with background activity in the Au foils. This background was observed by making a blank run with no target present, and is believed to be due to the $C^{12}(\alpha, Be^7)$ reaction, in thin deposits of pump oil on the hot surfaces of the foils, during long (up to 40 hours) bombardments. The high background activity makes the energy distribution somewhat uncertain.

Fig. 19-3 gives the angular distribution from the same run. The target thickness was 0.5 mg/cm^2 of Al. Since very few fragments were retained by the target itself, it is felt that target thickness did not greatly affect the angular distribution. The increase in $d\sigma/d\Omega$ at 160° is questionable, but the increase in forward direction is quite pronounced. The large error limit imposed on the point at 16° is due to the background difficulty mentioned above. A problem which remains is to ascertain the extent of oxygen and carbon contamination of the Al targets. The cross section for Be^7 production from oxygen or carbon is about ten

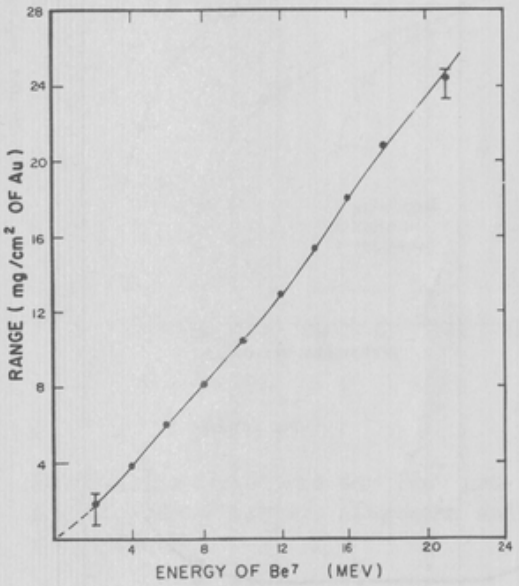

Figure 19-1

Range-energy relation for Beryllium-7 ions in gold. The error limits represent the uncertainty in extrapolating a range-difference curve. Intermediate points have similar error limits.

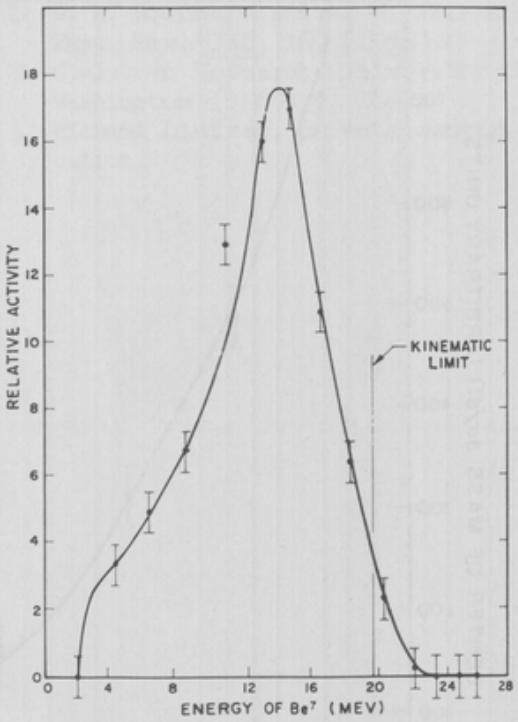

Figure 19-2

Energy distribution of Be^7 fragments from $Al^{27}(He^4, Be^7)$. Only forward moving Be^7 fragments in the angular range 0° to 16° were accepted.

times as great as for Al. Also the center-of-mass energy for the oxygen or carbon reaction is greater, and this would tend to enhance the forward peak. The angular distribution is not sensitive to the Be^7 energy selected from the momentum distribution.

The forward-backward ratio of Be^7 activity about 90° in the center-of-mass system is 2.5 to 1. Carbon or oxygen contamination of the Al target could have a large effect on this value.

Similar results have been obtained for Be^7 fragments from helium ion bombardment of oxygen, except that the forward-backward ratio is 1.2 to 1. We feel that more work is called for in order to distinguish between the several possible mechanisms for these reactions.

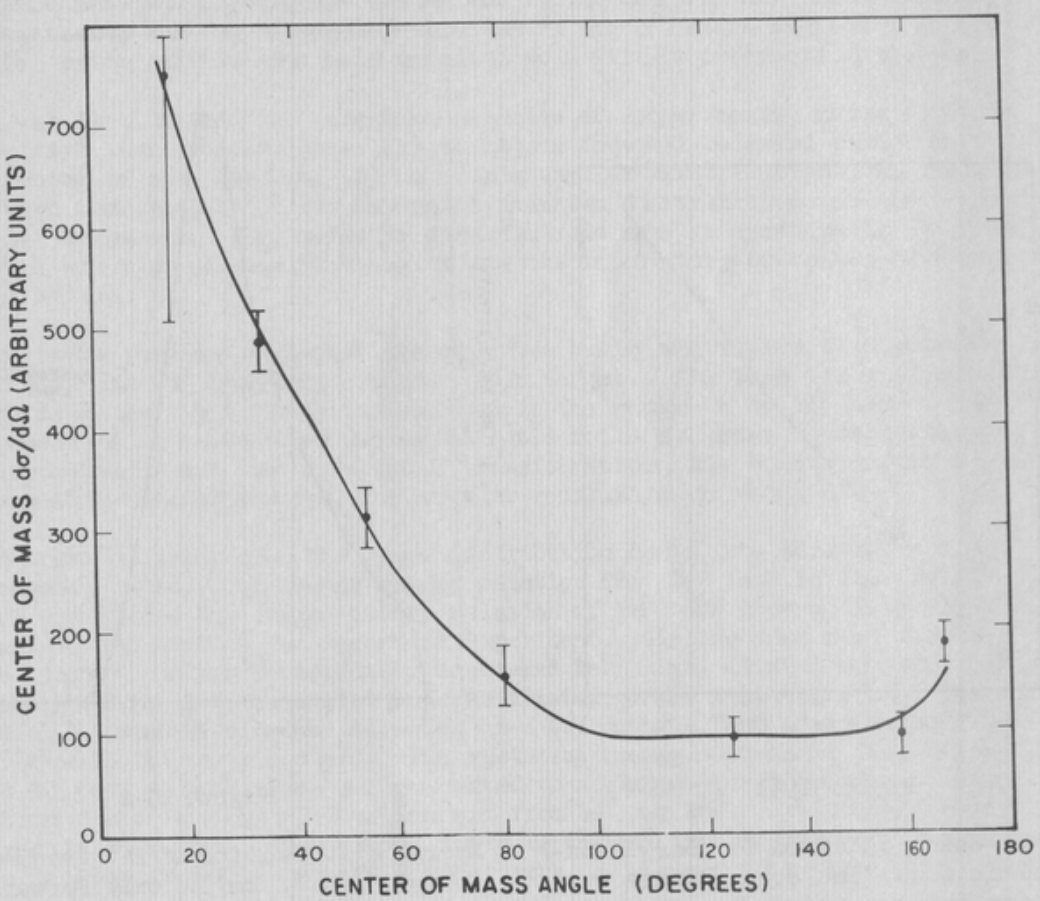

Figure 19-3

Angular distribution of Be^7 fragments from $Al^{27}(He^4, Be^7)$ in the center-of-mass system.

Fig. 19-4 presents excitation functions for Be^7 production from carbon, nitrogen, and fluorine bombarded with helium ions. (A. W. Fairhall, I. Halpern, and C. O. Hower)

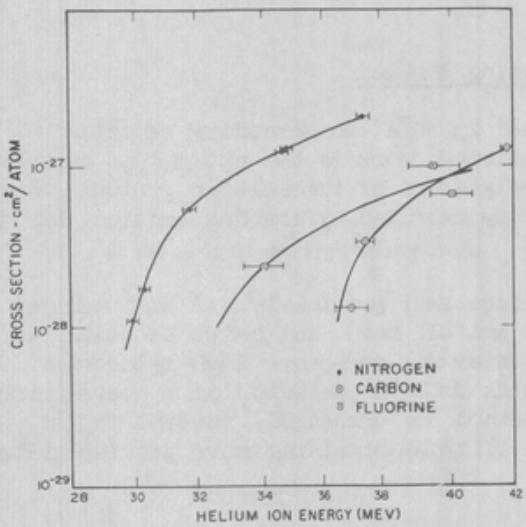

Figure 19-4

Excitation functions for Be^7 production from carbon, nitrogen and fluorine.

1 G. H. Bouchard and A. W. Fairhall, Phys. Rev. 116, 160 (1959).
2 Cyclotron Research, University of Washington (1960) p. 18.
3 Richard Lindsay, private communication.

V. COMPOUND NUCLEAR REACTIONS

20. Evaporation of Protons from Rapidly Rotating Nuclei

The study of proton evaporation, discussed in the two preceding reports,[1] is continuing. The main emphasis in this continued work is the attempt to obtain more detailed information on the angular correlations of the emitted protons, and thereby to determine, separately, the anisotropy carried by protons emitted early and late in the emission sequence.

The general method remains the same as discussed previously. A Ni^{58} target is bombarded with alpha particles (at 27, 32, and 42 Mev) and pairs of coincident protons are observed in scintillation counter telescopes. Each telescope uses a thin plastic "dE/dx" detector and a thick CsI "E" detector in a conventional dE/dx-E arrangement. Although the basic method is unchanged, several major changes have been made in the equipment to facilitate obtaining more precise data. These changes are:

(a) A new electronic system is employed for particle identification. Previously, the particle identification and energy determination were performed by displaying, on an oscilloscope screen, the pulse heights from all four detectors and separately analyzing photographs of the oscilloscope traces. This method is simple and unambiguous, but it is also tedious, and the pulse height distributions are not available until several weeks after completion of a run. The new method is analogous to the conventional multiplication method for particle identification, but addition is used instead of multiplication. Details of this adder system are given in Sec. 36.

(b) As discussed in the 1960 Progress Report,[1] one can learn about possible differences in the anisotropy of the two emitted protons by studying the angular correlation of particles emitted in the plane perpendicular to the incident beam. For this, one of the counters must have an azimuthal degree of freedom. To provide this, with accurate positioning of the counter, a new system has been designed and built. Details of the azimuthal rotation system are given in Sec. 42.

(c) The low energy threshold for proton detection, with virtually 100 per cent efficiency, has been lowered from 2.9 Mev to 2.3 Mev by using a thinner dE/dx detector (now 0.002") and a thinner aluminum light shield between the detectors.

Angular distributions obtained at 27 Mev and at 32 Mev are shown in Fig. 20-1. The curves in this figure represent an arbitrary fit to the experimental points at backward angles, and are continued symmetrically about 90° at forward angles. It is seen that the forward points lie somewhat above the symmetric curve, especially at 32 Mev. Such a front-back asymmetry is commonly ascribed to a direct interaction contribution; this appears to be a reasonable explanation in the present case. Preliminary data at 42 Mev suggest an even stronger forward peaking at this higher energy, and therefore, presumably, a larger direct interaction contribution. No quantitative estimate has yet been made of the magnitude of the possible direct component, but it is concluded from Fig. 20-1 and information on spectra and yields, that it is small at 27 and 32 Mev.

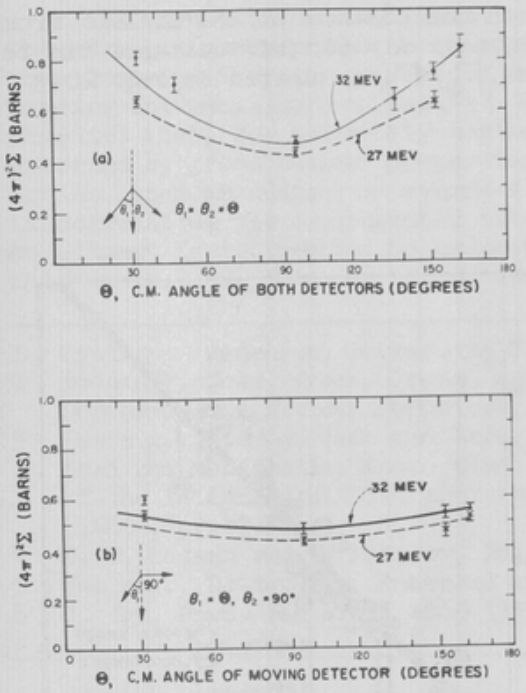

Figure 20-1

Differential cross sections (c.m.) for coincident proton events: (a) the two counters are symmetrically situated on opposite sides of the beam; (b) one counter is held fixed at 90°. Σ is the differential cross section in barns per steradian.[2] Σ is multiplied by $(4\pi)^2$ to give differential cross sections whose average is numerically equal to the total cross section.

The bulk of the cross section is here attributed, as previously, to compound nuclear evaporation. The 32-Mev yield is larger than the 27-Mev yield, presumably due to the higher total cross section for incident alpha particles and to the possibility of three particle emission at this higher energy.

Comparing the present results at 32 Mev with the results reported in the last report[1] and at the Kingston Conference,[2] it is to be noted that the magnitude and shape of the differential cross sections are in general agreement with the results obtained with the older system. However, there are several significant quantitative changes: (1) The cross section with both counters at 150° is lower than in the previous data. In addition to implying a possible direct interaction contribution, this suggests that the anisotropy in the compound nuclear evaporation is less than estimated previously, although still above the expectations for rigid body rotation. (2) The anisotropy when one counter is held at 90° and the other is moved, is also less than reported previously. The reasons for these discrepancies are not yet fully understood.

Very preliminary data on the angular correlation with both counters in the plane perpendicular to the beam is in agreement with earlier results showing a small, but not marked, variation of coincidence rate with azimuthal angle. Work is in progress to improve the precision of this data and to relate it to the results of the other anisotropy measurements reported above.

Observed energy distributions are shown in Fig. 20-2 for protons emitted at 90°. The spectra are seen to be quite similar at different incident alpha-particle energies. This is consistent with predictions of the statistical model, where only a weak dependence on incident energy is anticipated.

In addition to the angular correlation studies, an analysis has been made of the absolute proton yields in the (α, 2p) measurements reported previously for Ni^{58}, Ni^{60} and Ni^{62}. These yields can be compared with proton yields in (n,p) experiments at 14 Mev[3] and in (α,p) studies.[4] In general, it is expected that the ratio of the proton and neutron emission widths, Γ_p/Γ_n, depends primarily

on the proton richness of the nucleus, i.e., on the distance of the nucleus from the stable valley. In the region of interest, near A = 60, this distance can be represented by the term Z - 0.45 A. Therefore, Γ_p/Γ_n is plotted in Fig. 20-3

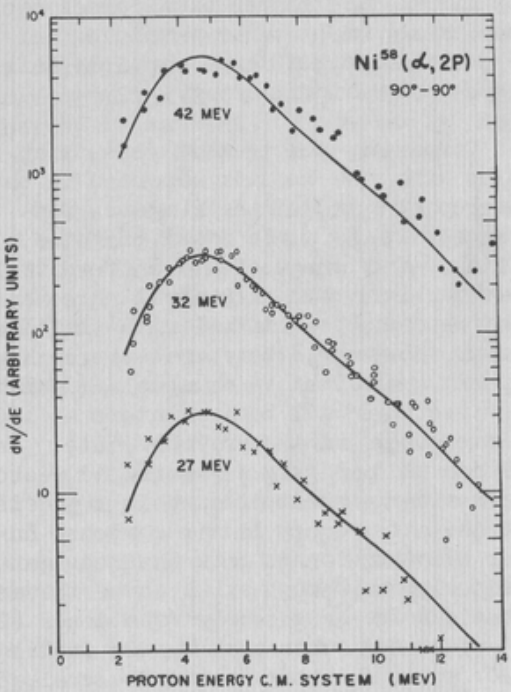

Figure 20-2

Energy distributions of coincident protons, at 90°, for various incident alpha particle energies. The points show the relative number of protons per unit energy interval in one counter when there is also a proton, of any energy, in the other counter. Energies and energy densities have been converted to the center-of-mass system. The solid curve, identical for the three cases, represents an empirical fit to the 32-Mev data.

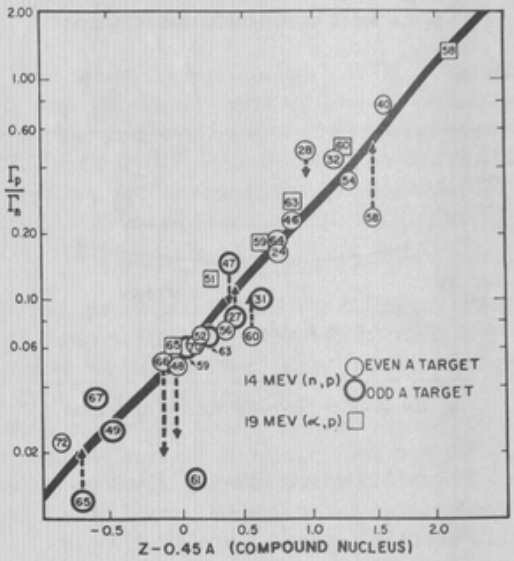

Figure 20-3

Dependence of the ratio of proton and neutron emission probabilities upon the distance from the stable valley, for incident neutrons and alpha particles. The data for incident neutrons is from a compilation by Facchini et al[3] (with arrows indicating cases where results of Storey et al[3] and Allan[3] give quite different results); the data for incident alpha particles is calculated from (α, p) cross sections of Lassen and Sidorov[4] and total cross sections of Igo.[6] The numbers within the symbols are the mass numbers of the target nucleus.

as a function of Z - 0.45 A, for the(n,p) and (α,p) measurements cited above. The experimental points are found to fall on a smooth curve, with relatively small scatter. Using this curve (a straight line) as a tool for predicting the proton yields in the present (α, 2p) experiments, it is found that the observed and predicted yields are in good agreement. This further supports the view that the protons involved are emitted from a compound nucleus.

The approach described here for studying Γ_p/Γ_n is somewhat equivalent to the more customary procedure of considering the specific binding energies and then removing the consequences of the ground state configurations by introducing pairing and shell corrections.[3,5] However, the present approach particularly emphasizes that, for moderately excited states, the emission probabilities are governed by gross nuclear properties, namely A and Z, and not by detailed properties, such as oddness or evenness. The character of the curve, and its success in correlating the experimental ratios Γ_p/Γ_n appears qualitatively reasonable. An attempt is in progress to understand quantitatively the slope and position of this curve. (D. Bodansky, C. R. Gruhn, I. Halpern, and R. West)

---

1 Cyclotron Research, University of Washington (1959), p. 29; (1960), p. 24.
2 Bodansky, Cole, Cross, Gruhn, and Halpern, Proceedings of the International Conference on Nuclear Structure, Kingston, Ontario, (1960), p. 749.
3 See e.g., Storey, Jack and Ward, Proc. Phys. Soc. 75, 526 (1960); Facchini, Iori and Menichella, Nuovo Cimento 16, 1109 (1960); D. L. Allan, Proceedings of the International Conference on Nuclear Structure, Kingston, Ontario, (1960), p. 838.
4 N. O. Lassen and V. Sidorov, Nuc. Phys. 19, 579 (1960).
5 See e.g., Dostrovsky, Fraenkel and Friedlander, Phys. Rev. 116, 683 (1959).
6 G. Igo, Phys. Rev. 115, 1665 (1959).

---

21. (α,p) Spectra and Angular Distributions with a Single Counter.

The preceding section describes the continuing investigation of the (α,2p) reaction in medium weight nuclei by means of the detection of pairs of coincident protons. There are a number of reasons for also making the more straightforward measurements of spectra and angular distributions with only a single detector. These include:

(1) This measurement complements the coincidence measurements by confronting any theoretical explanation of the coincidence angular correlations with a different type of angular distribution information.

(2) It allows one to study proton emission in neutron rich isotopes (where the yield of coincident protons is prohibitively small), and thus to explore the dependence of the ratio of emission widths, Γ_p/Γ_n, on proton richness (see preceding section).

(3) It allows one to see more clearly any direct interaction component in the proton spectrum. This component is harder to see in the coincidence experiment which discriminates against high energy protons by the demand for at least two particles.

(4) With a single counter one can afford to place the counter further from the target and thus explore more extreme angles. The theory seems to indicate that the yields at very forward or very backward angles are particularly sensitive to the values of the nuclear parameters which control the emission anisotropy.

For this purpose a counter system has been developed for the detection of single protons. The counter uses plastic and CsI phosphors in an arrangement which in general is similar to the one used for the coincidence experiment. However, it is designed to go to more extreme angles and the distance between the phosphors can be adjusted. In the single counter experiment, with detection thresholds set at low levels to accept protons over a wide energy range, one is particularly vulnerable to accidental coincidences from photon and neutron background events. (In the coincidence experiment such events are largely eliminated by the quadruple coincidence demands.) Special attention has therefore been given to attempts to improve the shielding arrangement and to finding a favorable place for the beam energy degrader. It has also been necessary to establish a moderately fast coincidence between the two detectors ($\sim$ 20 nanoseconds). The accidental events in general involve small pulses, and it has been found that it is easier to eliminate them with the x-y oscilloscope particle identification system (see Sec. 34) than with the adder system (see Sec. 36). The oscilloscope identification system is therefore being used to gate a 512-channel pulse height analyzer on which the proton spectrum is displayed.

The main effort, up to the present time, has been devoted to the development of the detection system. It is believed that the system is now satisfactory for studying proton spectra from 2.5 to 30 Mev without major background difficulties. Very preliminary data for the (α,p) reaction in Ni^{58} at 27 and 32 Mev show angular distributions with a minimum at 90° and spectra with relatively more high energy protons than in the coincidence experiment. These preliminary results appear qualitatively reasonable.

Work is continuing to obtain additional data on angular distributions and spectra of protons from Ni^{58} and other targets. (D. Bodansky, C. R. Gruhn, I. Halpern and R. West)

22. Neutron Time-of-Flight Studies

During the current year, development of the neutron time-of-flight spectrometer described previously[1] has continued. A number of significant improvements have been made, and encouraging results have been obtained in a number of varied tests. In fact, it has been possible to use the equipment for preliminary measurements of the spectra of neutrons emitted in bombardments with 42-Mev alpha-particles. The design permits quick and easy installation of the equipment. The apparatus consists of two main parts: the cyclotron beam modulator and the neutron detector.

The cyclotron beam modulator diverts two of every three consecutive bursts of the cyclotron beam. This permits the use of a flight path as great as 2 m without confusion in associating the neutrons with the proper burst. The energy resolution of the spectrometer increases with the flight path. The signal for the beam modulator originates in a frequency divider. This circuit receives a signal from the cyclotron oscillator and delivers an alternating potential with a frequency one-third as large, namely 3.9 Mcyc/sec. The frequency divider in use at present, designed by R. E. Karns, performs very satisfactorily.

The deflector plates of the modulator are located in the target box just outside the cyclotron. They are about one foot long and are one-half inch apart. Together with a coil, they form a resonant circuit which is driven to a peak voltage of 30 to 40 KV. The entire deflector system including these plates, the coil forming the rest of the tank circuit, and the driving circuitry was first developed and tested away from the cyclotron. When it operated satisfactorily, it was introduced into the cyclotron where two new insulation problems developed. The first was the electrical breakdown from the deflector plates to the target box walls. This was eliminated by surrounding the plates (except for beam openings) with a smooth copper jacket. The other problem was more serious. The high voltage insulator developed cracks due to local heating produced by charged particle bombardment. This problem was solved by replacing the earlier insulators by a large zircon insulator[2] (5-inch diameter x 6-inch length).

A set of slits which is part of the deflecting system is placed 4.5 m from the target box just ahead of the entrance into the water-filled shielding room. The diverted cyclotron beam bursts strike these slits. This separate set of slits is used rather than the already available duct slits so that the "wiping" may be accomplished as far from the cave area as possible in order to minimize background from the unused beam bursts. In the course of installing the wiping slits it was found that the major part of the beam passes through the duct near the focussing magnet within a very small (2-inch x 8-inch) area at its south end. The beam profile was conveniently surveyed by activating a 0.001-inch brass foil.

The beam modulator tests involved two kinds of detection. In one, the currents to the various slits and to the Faraday cup were read as a function of deflector voltage and phase between the cyclotron and the deflector subharmonic. This phase is continuously variable from the counting room by means of a variable delay line. The results were in good agreement with expectations. The most convincing results were obtained with a counter measuring protons scattered elastically from a polystyrene target. The proton pulses were delivered to the time-to-pulse-height converter. The stop signals for the converter were obtained from the cyclotron as described below. With the deflector off and the time base about 300 mμsec long, 3 sharp groups appeared in the time spectrum corresponding to successive cyclotron bursts. When the deflector was turned on, two of these groups were reduced to less than 0.1 per cent of their original size, while the third group was hardly affected.

We now turn to the detector system. A circuit to discriminate against photons in the neutron counter was built.[3] This circuit seems to work with reasonable efficiency for protons of energy greater than 0.7 Mev. The general photon background in the cave is, however, apparently, not too severe, and it may not be necessary to use this circuit. An auxiliary discriminator was built to precede the one in the start side of the time-to-pulse-height circuit. The new discriminator is fast and stable, and it has sharpened the time resolution of the circuit. Sharp discrimination is particularly important in time-of-flight work with fast neutrons (or photons), since here even monochromatic incident radiation gives rise to a very broad pulse height distribution in the detector. The methods of getting the "zero-time signal" from the Faraday cup or a monitor counter were abandoned when it was found that the signal from the cyclotron which drives the frequency divider can be made to provide a very sharp stable stop signal. The neutron detector operates around the 60-inch scattering chamber instead of its

own chamber as heretofore. For reasons of space and background, this arrangement has proved to be more convenient.

In testing the performance of the neutron detector, it has been convenient to use the elastically scattered 10-Mev proton beam and the reaction B^{10} (p,n) C^{10}. These reactions provide known monochromatic proton and neutron groups, and help to establish that the system is working properly. The main interest will be in neutrons from higher energy alpha-particle bombardments where the spectra are continuous rather than structured and do not themselves, therefore, provide easy tell-tale checks on the performance of the spectrometer. Neutron spectra have generally been measured by subtracting the background obtained when an absorber is placed between detector and target. A very preliminary neutron spectrum obtained by bombarding copper with 42-Mev alpha-particles is shown in Fig. 22. The lower curve is the time spectrum as it was recorded on the multichannel analyzer. The upper curve gives the corresponding neutron energy spectrum. It has not been corrected for the variation of detection efficiency with neutron energy. Such corrections would raise the low energy end of the spectrum slightly. The determination of the dependence of detection efficiency on neutron energy is one of the major remaining technical problems. Another involves the reduction in beam energy by means of degraders without creating intolerable amounts of background. It seems desirable to be able to reduce the incident energy, because the results are more readily interpreted when not too many particles are emitted in a reaction. One of the first experiments contemplated with the neutron detection system will be to study neutron energy and angular distributions from middle weight targets. It has been pointed out in earlier reports that a comparison of neutron and proton distributions can provide important information on the role of the coulomb field in determining the emission directions of outgoing particles. This, in turn, might reveal how the particle evaporation flux depends on the latitude (with respect to the rotation axis) of the emitting area on the surface of the nucleus. (D. Drake and I. Halpern)

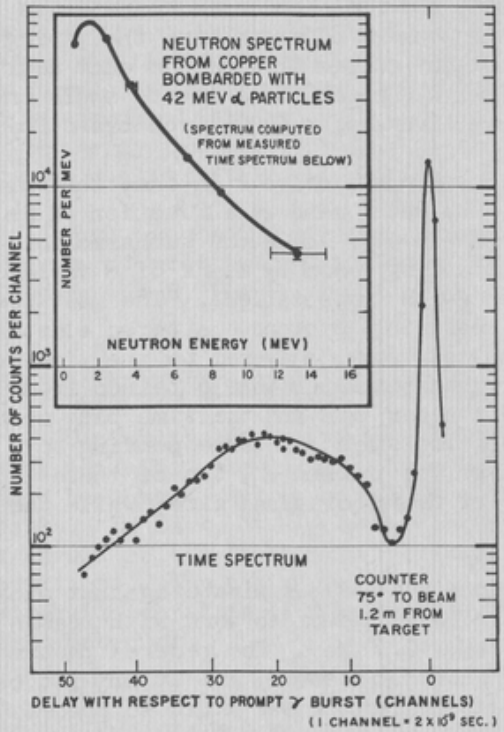

Figure 22

Neutron time and energy spectra in bombardment of Cu with 42-Mev alpha particles.

1 Cyclotron Research, University of Washington (1960), p. 47.
2 Made by Coors Porcelain Company, Golden, Colorado.
3 W. Daehnick, private communication.

VI. MISCELLANEOUS NUCLEAR REACTIONS

23. The Circular Polarization of Photons From Nuclear Reactions

This experiment was discussed in two previous reports.[1] It consists of simultaneous detection of inelastically scattered particles and de-excitation gamma-rays after the latter have been passed through a magnetized iron polarization analyzer. The difficulties with the experiment stemmed from the originally poor duty cycle of the cyclotron and high background radiation. However, with the reduction in background brought about by the dee-voltage regulator (see Sec. 29), plus several additional paraffin and cadmium shields in the beam duct system, another attempt was made to determine the feasibility of the experiment.

The results show that the desired coincidences are present with a signal-to-background ratio of about ten. Understandably, the coincidence rate is very low, and it is estimated that from two to three weeks of continuous operation would be required to collect a significant number of counts. It is tentatively decided to abandon this experiment, at least until the demand for cyclotron operation time has diminished. (J. B. Gerhart, W. A. Kolasinski, and F. H. Schmidt)

---

1 Cyclotron Research, University of Washington (1959), p. 7; (1960), p. 23.

---

24. Spin-Flip in Inelastic Scattering

When an even-even nucleus (0+ ground state) is excited to a (usual) 2+ first excited state by means of inelastic alpha-particle or proton scattering, the amplitudes of the various "m" states excited are determined by the details of the reaction mechanism. For convenience the perpendicular to the reaction plane is taken as the direction of quantization. When alpha-particles are scattered, then only $m = 0$ or $m = \pm 2$ states can be excited.[1] The gamma-radiation patterns from these states exhibit zero intensity in the direction perpendicular to the reaction plane. On the other hand, for proton scattering, $m = \pm 1$ states may be excited if the proton undergoes spin-flip in the scattering process. Subsequent gamma-radiation from these $m = \pm 1$ states is most intense in the direction perpendicular to the reaction plane.

The experimental arrangement was described in the previous report.[2] This work is continuing with improved counters, and with reduced gamma-ray background (See Sec. 29). To date, runs have been made on C^{12} (p, p'γ) and Mg^{24} (p,p'γ). The first reaction produces substantial spin-flip, while the latter appears to produce very little. Quantitative statements cannot be given until a calibration of the gamma-ray detector has been obtained; this will be accomplished by studying the angular correlation in the reaction plane. This has necessitated a newly designed gamma-ray detector which is suitable for operation inside the evacuated 60-inch scattering chamber. (J. B. Gerhart, W. A. Kolasinski, and F. H. Schmidt)

---

1 A. Bohr, Nucl. Phys. 10, 486 (1959).
2 Cyclotron Research, University of Washington (1960), p. 23.

---

25. Investigation of (α,p) Nuclear Reactions

These reactions have been discussed previously.[1] The angular distributions of protons from the $C^{12}(\alpha,p)\ N^{15}$, $Al^{27}(\alpha,p)\ Si^{30}$, and $P^{31}(\alpha,p)\ S^{34}$ reactions were studied at 42 Mev.[2] The initial motivation for the study was to determine whether the angular distributions showed a parity-sensitive structure. Both the ground state and the third excited state protons for the $C^{12}(\alpha,p)\ N^{15}$ reaction show pronounced diffraction-like patterns, as shown in Fig. 25-1. However, in

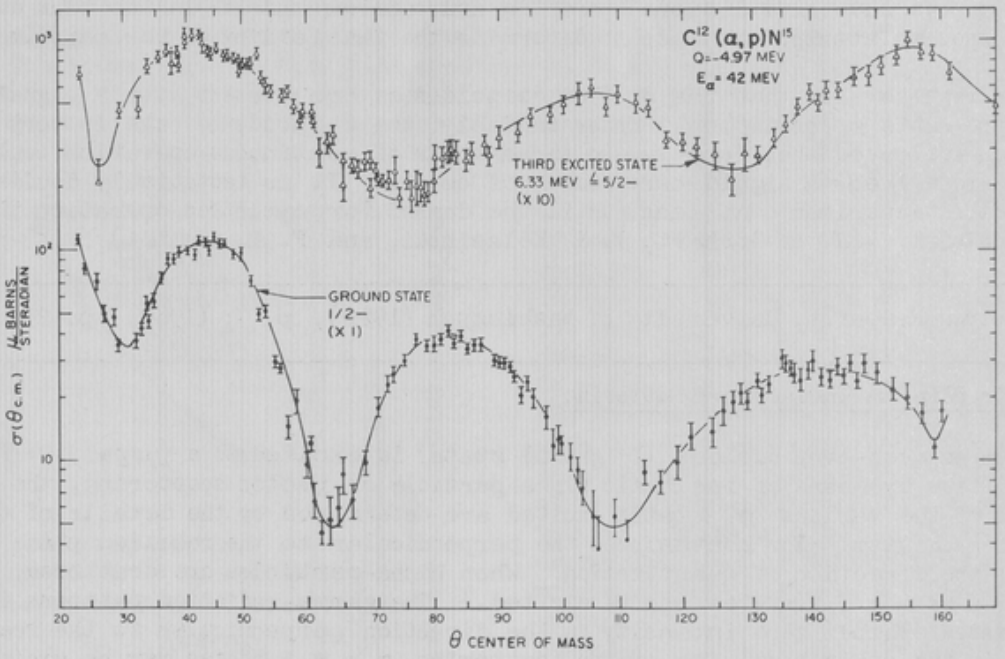

Figure 25-1

Angular distributions of protons from the ground state transition and third excited state in the reaction $C^{12}\ (\alpha,p)\ N^{15*}$.

contrast, neither the ground state nor the first excited state groups for the $Al^{27}(\alpha,p)\ Si^{30}$ reaction show any marked structure, as may be seen from Fig. 25-2. Fig. 25-3 shows the angular distribution for the $P^{31}\ (\alpha,p)\ S^{34}$ reaction. The difference between these last two reactions may be explained by the shell model: The last proton is loosely bound in P^{31} in the $2s_{1/2}$ shell; while in Al^{27} the protons lack one particle of completing the $1d_{5/2}$ shell. The phasing of the various diffraction-like angular distributions does not agree with that expected on the basis of parity arguments alone. Attempts to fit the distributions with the theoretical predictions of various direct interaction mechanisms have met with only partial success. The agreement is particularly poor for the excited state reactions.

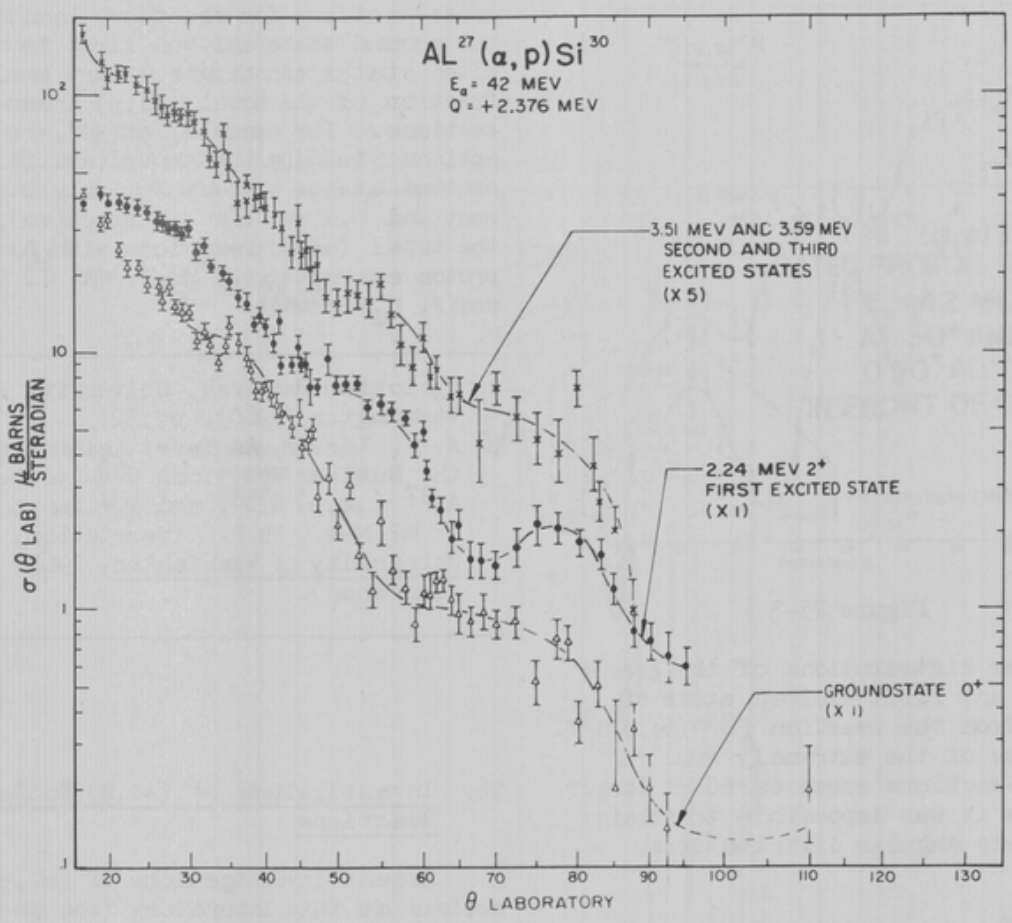

Figure 25-2

Angular distributions of the first four states of Si^{30*} from the reaction Al^{27} (α,p) Si^{30*}.

The experiment was performed in the 60-inch scattering chamber, utilizing a double scintillation counter which distinguished protons from other reaction products. A "dE/dx" pulse was derived from a thin plastic scintillator, and an "E" pulse from a CsI (Tl) scintillator. The two spectra were displayed on twenty-channel analyzers by the "cross-gating" technique. Particular care was required in order to achieve separation of the various proton groups. Under the best of conditions resolutions of 1.2 to 1.5 per cent in energy were obtained for the highest energy protons ($\sim$ 30 Mev). In addition, the differential cross-section for which reliable data was obtained is 0.5 μbarn/steradian.

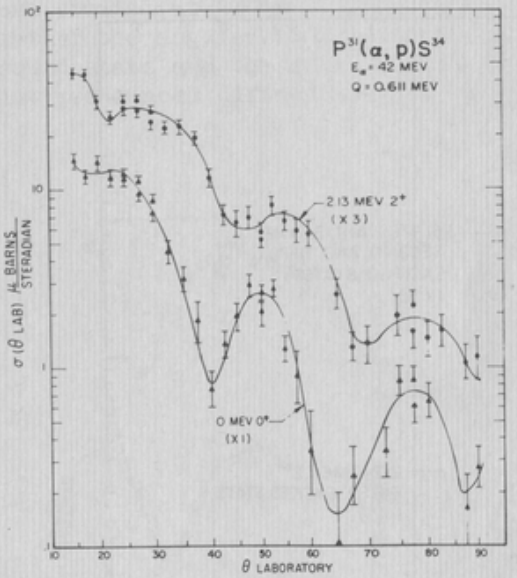

Figure 25-3

Angular distributions of the ground state and first excited state of S^{34*} from the reaction P^{31} $(\alpha,p)S^{34*}$. Because of the extremely small cross-sections encountered at larger angles it was impossible to obtain complete angular distributions.

At a few angles the proton spectra were measured at energies as low as 5 or 10 Mev. A typical curve is shown in Fig. 25-4. It is noteworthy that the cross-sections for reactions leading to the ground state and the first few excited states constitute a very small fraction of the total (α,p) cross-sections. For example, at 30°, reactions yielding the ground and first excited states account for only 0.06 per cent and 0.1 per cent, respectively, of the total (α,p) reactions with Al^{27} for proton energies >5.5 Mev. (A. J. Lieber and F. H. Schmidt)

---

1 Cyclotron Research, University of Washington (1960), p. 32.

2 A. J. Lieber, An Investigation of the Nuclear Reactions C^{12} (α,p) N^{15}, Al^{27} (α,p) Si^{30}, and P^{31} (α,p) S^{34} at 42 Mev., Ph.D. dissertation, University of Washington, 1961, (unpublished).

---

26. Investigations of (α,d) Nuclear Reactions

Recent investigations of (α,p) reactions at this laboratory (see Sec. 25) have indicated that a lack of a diffraction like angular distribution may possibly be interpreted in terms of the shell model, by associating a diffraction pattern with a loosely bound proton. Similar considerations may also apply to (α,d) reactions, using two-nucleon stripping or knockout theories, where the availability of a loosely bound deuteron could again be given by the shell model. On the other hand, the cluster model might also be expected to provide a suitable basis for the interpretation of (α,d) reactions.

Studies of angular distributions in (α,d) reactions are being undertaken to determine the extent to which shell model or cluster model interpretations may be appropriate. At present, reactions with Li^6, C^{12}, and N^{14} targets are being studied. The counter telescope used in the (α,d) work is being used in conjunction with an (x,y) oscilloscope particle identification system (see Sec. 34). In addition, a proportional dE/dx counter is being developed for (α,d) studies at low deuteron energies, where the necessity for a thin dE/dx detector makes it difficult to separate protons and deuterons in a scintillation counter. (F. H. Schmidt and C. D. Zafiratos)

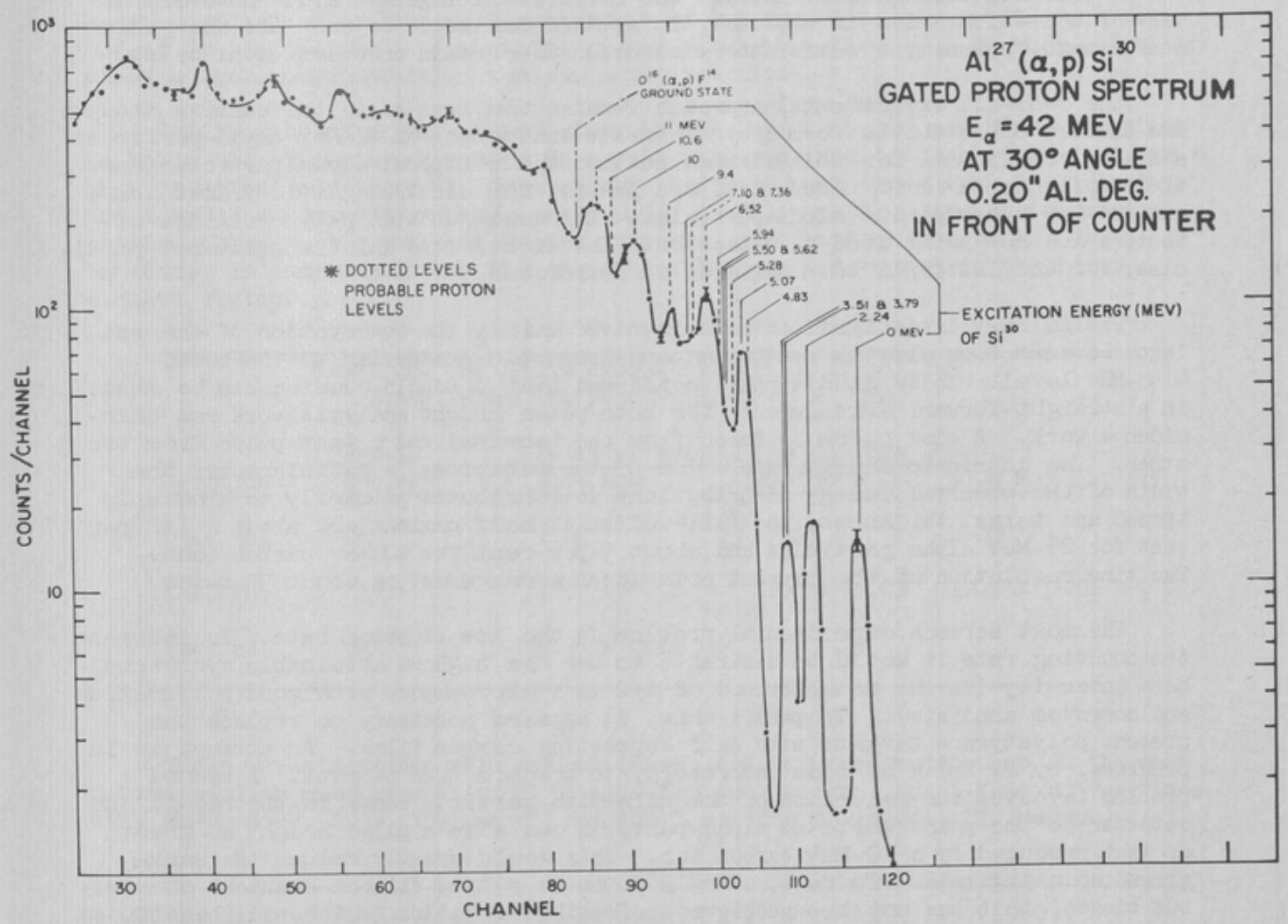

Figure 25-4

Proton spectrum at 30° from the reaction $Al^{27}(\alpha,p)Si^{30*}$. The calculated positions of the excited states of Si^{30*} are indicated at the top of the figure. The dotted lines indicate the positions of probable levels.

27. Breakup of C^{12*} (7.66 Mev)

In an earlier study at this laboratory of the decay of C^{12} from the excited state at 7.66 Mev, it was concluded that the width for electromagnetic transitions to the ground state is less than 0.1 per cent of the width for breakup into alpha-particles[1]. The advent of solid state detectors, with their good energy resolution for heavy particles, has stimulated an attempt to extend this measurement, and, if possible, to determine the ratio of the radiative and alpha-particle widths. Subsequently, a measurement of this ratio has been reported by Alburger,[2] who has studied coincidences between the de-excitation gamma-rays. However, in view of the differences in approach, it appears desirable to continue the present measurement, assuming a satisfactory solution to certain problems cited below.

The over-all experimental approach remains the same as in the earlier study. The excited C^{12} state is formed by inelastic scattering of 42-Mev alpha-particles, and a search is made for coincidences between the scattered alpha-particles and the recoil carbon ions. These ions are present for electromagnetic transitions, but not for breakup into alpha-particles. Diffused junction p-type silicon detectors are now being used to detect both the carbon ions and the scattered particles; for the latter, a thin degrader is introduced.

Preliminary investigations have involved mainly the observation of the analagous events from elastic scattering and inelastic scattering to the bound 4.43-Mev level. These studies have confirmed that a single counter can be used, in a straight-forward arrangement, for both pulse height analysis work and coincidence work. A slow pulse is taken from one terminal and a fast pulse from the other. The intrinsic energy resolution of the detectors is satisfactory; the width of the observed energy distributions is attributed primarily to kinematic spread and target thickness; the full-widths at half maximum are about 2 1/2 per cent for 25-Mev alpha particles and about 7 per cent for 10 Mev carbon ions. The time resolution of the present coincident arrangement is about 30 mμsec.

The most serious experimental problem is the low counting rate. To increase the counting rate it would be desirable to use the highest attainable cyclotron beam intensity (in the neighborhood of 1/2 to 1 microampere with good collimation and momentum analysis). To permit this, it appears necessary to replace the present polystyrene targets with self supporting carbon films. An attempt is in progress, by P. Kelsh of this laboratory, to prepare such targets. A second problem involves the reduction of the effective particle range in the recoil ion detector to the point where no alpha-particle can give a pulse height as great as that produced by a 10-Mev carbon ion. This would greatly reduce the background counting rate. To date, using 300 ohm-cm p-type silicon counters at various biases, this has not been achieved. Possible solutions which will be studied include reduction of bias to very low levels, reduction of input time constants, or use of lower resistivity silicon. (D. Bodansky and C. R. Gruhn)

---

1 S. F. Eccles and D. Bodansky, Phys. Rev. 113, 608 (1959).
2 D. E. Alburger, Bull. Am. Phys. Soc. Ser II, 6, 226 (1961).

---

28. A Study of (α, xn) Reactions Through Observations of the Recoiling Nucleus

Harvey, Wade, and Donovan have measured the ranges of the recoiling nuclei produced in the Bi^{209} (α, xn) reactions.[1] It was found that for energies near 40 Mev, the (α, 4n) and (α, 3n) reactions apparently proceed with the formation of a compound nucleus, while the (α, 2n) reaction does not involve this type of mechanism. It has also been shown that the reactions K^{41} (α,n) Sc^{44} and Mn^{55} (α,n) Co^{58} proceed at least in part without forming a compound nucleus.[2] The nature of such reactions that proceed without the formation of a compound nucleus will be clarified by measurements of the ranges of the recoiling nuclei, and it is planned that a systematic survey along this line will be made. Similar studies are contemplated for the (α,α xn) reactions.

The results of a preliminary study of the Cu^{65} (α, xn) reactions are given in Table 28. The average ranges in copper were measured by techniques that have been described elsewhere.[2] These results indicate that the (α,n) reaction does not involve a compound nucleus, while the (α, 2n) reaction appears to proceed entirely through the compound nucleus process. The latter observation is interesting in comparison with the studies of Donovan and others in the heavy element region.

Table 28. Relative Average Ranges of Recoiling Nuclei From the Reactions Cu^{65} (α, xn)

Reaction	Recoil Nucleus	Relative Range for α-Energy Shown		
		41.4 Mev	40.0 Mev	38.4 Mev
(α, 3n)	Ga^{66}	1.00	1.00	1.00
(α, 2n)	Ga^{67}	1.00 ± 0.01	1.06 ± 0.03	1.05 ± 0.01
(α, n)	Ga^{68}	0.75 ± 0.02		

These investigations will be continued, and it is expected that in the near future similar measurements will be made for the (α, xn) and (α, αxn) reactions with Mn^{55}, Co^{59}, As^{75}, Y^{89}, Ag^{107} and Au^{197} as target nuclei. (T. Matsuo)

1 G. B. Harvey, W. H. Wade and P. Donovan, Phys. Rev. 119, 225 (1960).
2 T. Matsuo and T. T. Sugihara, Can. J. Chem. 39, 697 (1961); T. Matsuo and T. T. Sugihara, Annual Progress Report, Contract AT(30-1), 1930 (1961); T. Matsuo, "Formation of the Nuclear Isomers of Scandium-44 and Cobalt-58 by the (α,n) Reaction," Ph.D. thesis, Clark University, 1961 (unpublished).

VII. CYCLOTRON DEVELOPMENT AND RESEARCH

29. Reduction of Background in Nuclear Reaction and Scattering Experiments With the Dee-Voltage Regulator[1]

The purpose of this section is to discuss the origin and reduction of background counts arising in nuclear reaction or scattering experiments. Particular reference is made to particle-particle and particle-photon coincidence experiments. The very feasibility of a prospective experiment may rest upon obtaining good signal-to-background ratios, coupled with reasonable counting rates. By means of a regulator[2] for holding the dee-voltage constant and ripple-free, we have achieved, for certain types of experiments, a several-fold reduction of general background radiation in the 60-inch scattering chamber. In addition, the regulator has increased the duty cycle of the beam by a factor which varies between three and ten, depending upon operating conditions. For constant signal-to-background ratios, counting rates are multiplied by the same factor. The regulator has thus broadened the scope of possible experiments.

Consider first a coincidence experiment that requires the simultaneous detection of two particles, either heavy particles or photons. If the incident beam is contained in pulses of a duration less than the resolving time of the coincidence circuit, and with an interval between pulses greater than the resolving time, then the accidental coincidence rate is $(N_1N_2/f)\left[(Q^2)_a/Q_a^2\right]$; here N_1 and N_2 are respectively the individual counting rates, f is the frequency of the beam pulses, Q is a measure of the individual beam pulse size, and Q_a indicates an average. The second fraction is unity if the pulses are uniform; otherwise it is larger. It indicates the importance of the time-distribution of the beam. The cyclotron beam has a pulse duration of $\sim 5 \times 10^{-9}$ sec. and a pulse frequency $f = 10^7$/sec.; hence a reasonably fast coincidence circuit fulfills the conditions mentioned above.

Radiation which is recorded by the counters and which has a random distribution in time also contributes to the accidental coincidence rate. A conspicuous example has been the gamma-radiation excited when the beam strikes nearby slits or beam-catchers, or when neutrons interact with adjacent material, etc. If N_1' and N_2' are the corresponding increases in the individual counting rates, then the corresponding contribution to the accidental coincidence rate is $2\tau(N_1N_2' + N_2N_1' + N_1'N_2')$, where τ is the resolving time of the coincidence circuit. To make this correction it is necessary to distinguish N_1' from N_1 and N_2' from N_2; this requires the determination of the time-distribution of the beam and other parameters, and is usually a formidable undertaking.

In experiments involving only a single detector, background problems may still be serious. Two events, neither of which would be recorded alone, may occur within the same beam pulse and "pile-up" to produce a count. If the decay time of the detector is longer than the pulse duration, but shorter than the interval between pulses, then the corresponding contribution to the counting rate is $A(N'^2/f)\left[(Q^2)_a/Q_a^2\right]$ where N' is the rate at which such individual signals are received by the detector, and A is a factor which depends on their distribution in pulse size. Here again the time distribution of the beam plays an important role. Again, the roughly steady radiation which forms a general background

existing between pulses can cause pile-up accidentals equal to $A\tau N^2$, where τ is now an effective dead-time for the detector.

A common technique for measuring the accidental coincidence rate is to delay the pulses from one counter by a time equal to one cyclotron period. This method is satisfactory if the fractional variation of pulse size in consecutive beam pulses is small, but if this condition is not satisfied, the accidental coincidence rate is underestimated. Most measurements of this type for the energy-analyzed beam from the cyclotron indicated that $(Q^2)_a/Q^2_a > 3$, thus demonstrating that the duty cycle of the beam was probably bad. Fauska, Orth, and Schmidt[2] found by direct measurement that this was indeed true, and that fluctuations were to be attributed primarily to the poor regulation of the dee-voltage. To improve the duty cycle of the beam, an electronic regulator was constructed to maintain the dee-voltage. To improve the duty cycle of the beam, an electronic regulator was constructed to maintain the dee-voltage constant and ripple-free. This unit has been in constant use for over a year.

The original motivation to improve the duty cycle of the beam derived from proposed experiments on inelastic scattering of alpha-particles and protons with coincident detection of the de-excitation photons (see Sec. 23, 24). Initial tests had shown that the background gamma-radiation coming from a defining slit placed in front of the target was several times more intense than the desired radiation from the target. Yet the defining slit was necessary in order to obtain a sufficiently narrow focussed beam. With dee-voltage regulation, on the other hand, the undefined beam is well focussed, so that no slits are required. The effect of the regulator on the focussed beam image has been presented previously.[2] Removal of the defining slit in front of the target eliminated the primary source of background gamma-radiation. For example, in the C^{12} $(p,p'\gamma)$ reaction with 11-Mev protons, the background gamma-radiation is less than 1 per cent of the primary radiation for pulse heights above 1 Mev in a NaI(Tl) counter. For the C^{12} $(\alpha,\alpha'\gamma)$ reaction this ratio is less than 2.5 per cent. We emphasize that without the dee-voltage regulator these ratios are 200 per cent or more.

For experiments involving detection of a heavy particle, a defining slit is generally not objectionable. In these experiments, the primary effect of the regulator is to reduce the number of pile-up counts by a factor of three or more.

For particle-particle coincidence experiments the primary effect of the regulator is the improvement of the duty cycle of the beam. In $(\alpha, 2p)$ and similar reaction studies[3] in which the outgoing protons are detected in coincidence, Bodansky, et al[4] now obtain near agreement between measured accidental coincidence rates (obtained by delaying pulses from one counter one cyclotron period) and rates calculated by the formula N_1N_2/f, based on the assumption that $(Q^2)_a/Q^2_a = 1$. Before the regulator was installed, they obtained measured rates three or more times greater than the calculated value.

For particle-photon coincidence experiments similar improvements have been found. In a recent measurement on the C^{12} $(p,p'\gamma)$ reaction, the measured proton-photon accidental coincidence rate was about 20 per cent less than the value calculated by the formula N_1N_2/f. This indicates that, as expected, some photons reach the counter during the time between beam pulses so that the photon counting

rate is too high. Further, in an experiment in which the photons were Compton-scattered before detection in a NaI(Tl) counter (and thus greatly attenuated) the measured accidental coincidence rate was more nearly equal to the value calculated from $2\tau N_p N_\gamma$, rather than that given by $N_p N_\gamma / f$; in this experiment 2τ = 15 mμsec. This shows clearly that most accidentals in this case are caused by backscattered radiation which is random in time. Had it been necessary to define the beam in front of the target, as was necessary without the dee-voltage regulator, this random radiation would overwhelm completely the true coincidences.

We can summarize the improvements brought about by the dee-voltage regulator as follows: (1) The quality of single particle detection experiments has been improved and the operating time required for them has been substantially reduced, primarily by reduction of pile-up. (2) For particle-particle coincidence experiments, the main gain is derived through the improved duty cycle of the beam. For given counting rates this factor is three or more. (3) For detection of gamma-rays only, the regulator is absolutely essential. (4) For particle-photon coincidence experiments, the reduction in background is five-fold or more, and the range of possible experiments is substantially broadened. (H. Fauska, J. Orth and F. H. Schmidt)

---

1 Excerpts from paper (NE/155) submitted to the International Conference on Nuclear Electronics, Belgrade, Yugoslavia, May 15-20, 1961, by F. H. Schmidt, H. Fauska, and J. Orth.

2 H. Fauska, J. W. Orth, and F. H. Schmidt, Fixed Frequency Cyclotron Operation with a Regulator for Dee Voltage Stabilization, Nuc. Instr. and Methods, 10, 73 (1961). Cyclotron Research, University of Washington (1960), p. 35, 36.

3 See Section 20.

4 D. Bodansky, private communication.

---

30. Frequency Stabilization and Grid Current Control in the Cyclotron Oscillator

From a study of the fluctuations of the cyclotron beam current it became clear that they were to be attributed in part to the variations of the oscillator frequency. Accordingly, a system was developed to stabilize the frequency. A block diagram is shown in Fig. 30-1.

The signal from a transistorized crystal-controlled local oscillator is mixed with a signal from the cyclotron oscillator to produce a beat signal with a frequency of about 1 Mcyc/sec. This signal is, in turn, mixed with the signal from a variable oscillator to produce a beat signal with a frequency of about 10 Kcyc/sec. This signal is introduced into a frequency detector whose output is amplified by a low-drift differential amplifier that feeds a pair of Schmitt trigger circuits, each of which excites a relay. The relays control the mechanical adjustment of the compensators and hence the frequency of the main oscillator. Thus the operator regulates the cyclotron frequency by setting the frequency of the adjustable oscillator. To prevent overcorrection, a pulsed relay is employed

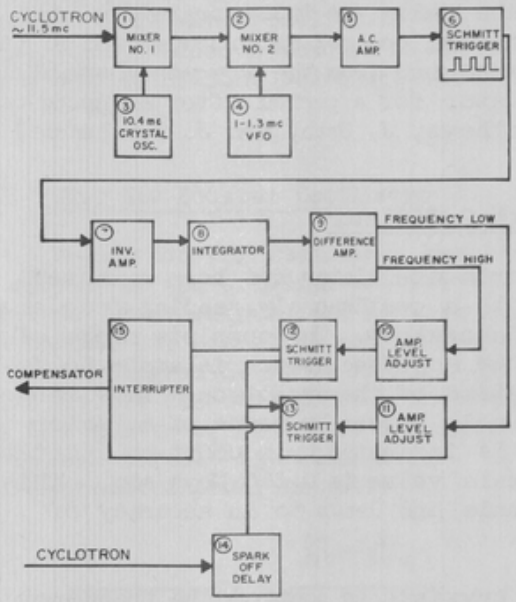

Figure 30-1

Block Diagram of the Frequency Control System.

which restricts the motion of the compensators to short-well separated intervals. Another circuit keeps the relays inactive during sparking in the main oscillator circuit, that is, in the cyclotron. This device has an adjustable time delay, which may be set for several seconds, which delays the corrective action and allows the main oscillator to recover and return to steady operation after a spark.

When the frequency stabilizing unit was put into operation, about Dec. 1, 1960, it was found that its corrective action also produced a change in the grid current of the main oscillator. Therefore a system for stabilizing the grid current was developed. A block diagram is shown in Fig. 30-2.

The signal from an alternating current (60 cyc/sec) bridge circuit, which includes a saturating transformer in the grid circuit of the main oscillator, is rectified and then combined in opposition with a direct-current reference voltage which is adjusted at the control console.

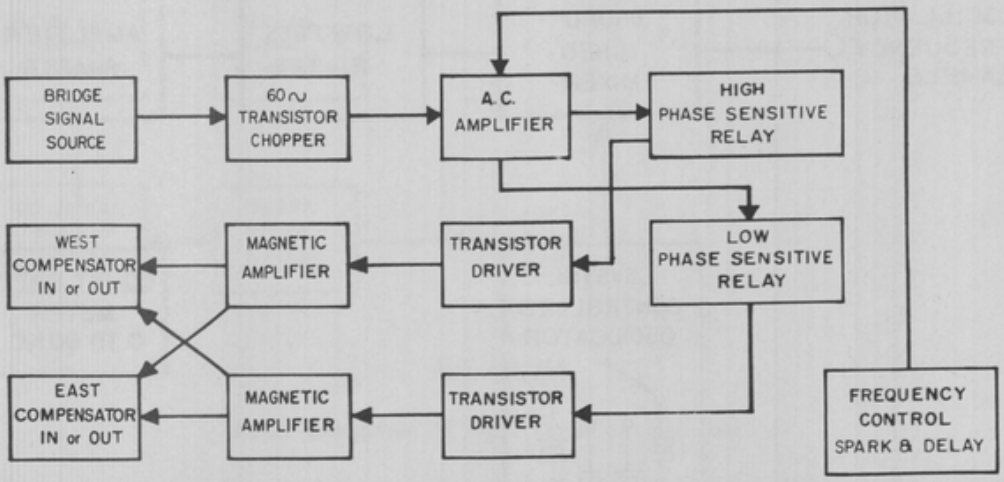

Figure 30-2

Block Diagram of the Grid-Current Control System.

Any resultant voltage constitutes the error signal, and is introduced into a transistorized chopper circuit, and the resulting square wave is amplified and applied to a pair of phase-sensitive circuits, each of which operates a relay.

In order to reduce the noise in the counting equipment and to eliminate relay chatter, a magnetic amplifier controlled by the relay was incorporated in the line for each compensator driving motor. A manual control is provided which can over-ride the automatic regulation system. A signal from the frequency stabilizing system deactivates the grid current regulator for a period after a spark occurs in the main oscillator circuit. (R. Matthews, J. Orth, and J. Turneaure)

31. A New Frequency Monitor for the Cyclotron Oscillator

In the past, the frequency of the cyclotron oscillator has been measured with a wave-meter. This has been replaced with a continuously reading frequency indicator, designed and constructed in this laboratory. The complete range of frequencies accessible is from 11.400 to 11.600 Mcyc/sec, which is ample to include the variations encountered in the operation of the cyclotron. This range is divided into four equal bands, of which one is chosen by means of selector switch. Within the selected band, frequency is indicated by a count-rate meter, mounted on the control console, whose full-scale value is 0.060 Mcyc/sec. This value provides some overlap among the four bands and leads to an accuracy of ±0.002 Mcyc/sec, which is quite satisfactory.

The selector switch selects one of four crystals to control the frequency of a local oscillator whose signal is mixed with that from the cyclotron oscillator. The resulting beat signal is shaped and introduced into the count-rate meter. A block diagram is shown in Fig. 31. The entire device is transistorized. It has been in constant use for seven months, and has given dependable and trouble-free service.

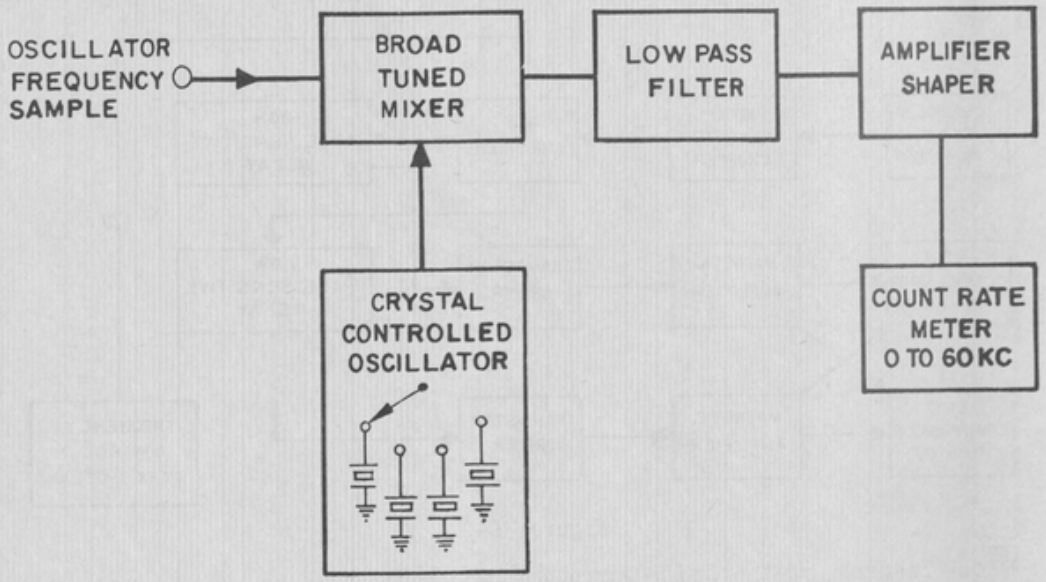

Figure 31

A Block Diagram of the Frequency Monitor

By providing continuously to the operator information on the oscillator frequency, this unit facilitates the efficient operation of the cyclotron. It is especially valuable when it is necessary to reproduce the conditions of operation in a series of runs which may occur during a period of several weeks. (H. Fauska and R. Karns)

32. The New Booster Oscillator

A new booster oscillator has been constructed. It accomplishes the same purposes as the original booster oscillator, but it has improved stability and a greater power output, and is more conveniently arranged for maintenance and adjustment. It has given continuous and satisfactory service for about six months. A block diagram is shown in Fig. 32. One important innovation of the new arrangement is the use of a pulse modulation circuit. An alternating voltage is applied to the plates of the power amplifier, and the high voltage rectifiers of the original circuit are eliminated. Consequently, there is a large increase in the instantaneous power output.

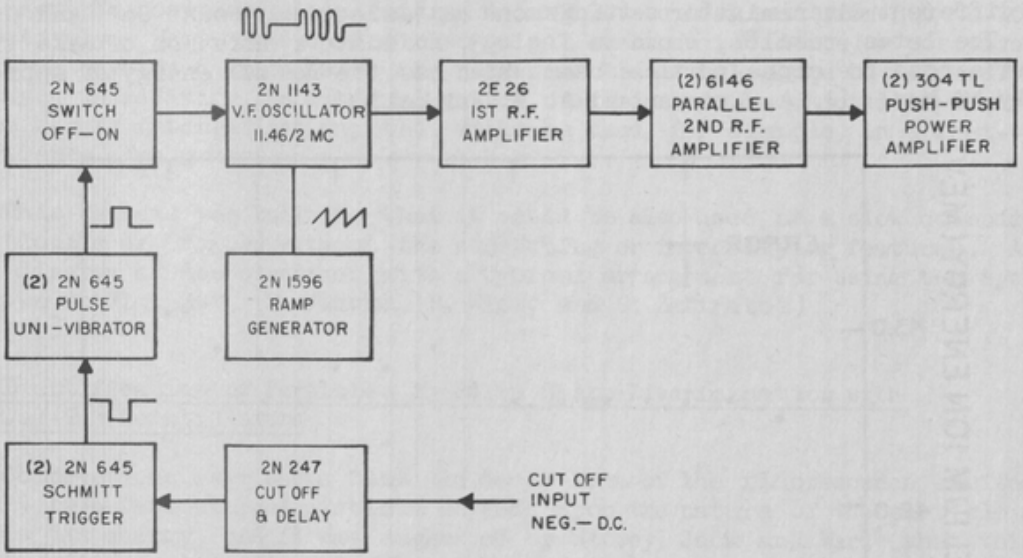

Figure 32

Block Diagram of the Booster Oscillator

The power amplifier section (a push-push doubler) and the master oscillator are built on separate chassis for convenience in dismantling for servicing. The low voltage plate power supply and the bias voltage supply are on a separate chassis equipped with interlocks to protect the power tubes from loss of bias. Metering equipment on the front panel indicates the currents in the two amplifiers, the output voltage, and the bias voltages. Controls on the chassis permit adjustments of the frequency modulation band width, the center frequency, the pulse width, the cut-off threshold, and the cut-off delay. The new booster

exploits recent developments, such as the use of "Vari-Caps" for frequency modulation, transistorized circuits, and Zener-diode biasing. The complete system is contained in a well shielded and well ventilated rack on the balcony near the main oscillator. A new coupling loop and new terminating capacitors have been installed at the termination of the transmission line. (R. Karns and J. Orth)

33. The Energy Inhomogeneity of the Helium Ion Beam

The method of Porile and Morrison[1] has been adopted to study the variation of the alpha-particle energy across the 10 cm width of the cyclotron beam in the target box used for routine irradiations. Thin copper foils are placed in the beam path for several minutes, cut into segments, and counted. The principle reaction products are Ga^{66}, Ga^{67}, and Cu^{64} produced respectively by the $Cu^{65}(\alpha, 3n)$, $Cu^{65}(\alpha, 2n)$, and $Cu^{63}(\alpha, 2pn) + Cu^{65}(\alpha, \alpha n)$ reactions. A ratio of gross activity measured one day and six days after the irradiation is related to the incident particle energy by the relative size of the cross sections of the dominant reactions. Beta proportional counting has proved to be unreliable. Presently the Cu foils are analyzed for gamma radiation in a well crystal. By using different discriminator settings one can selectively count Ga^{67} and $Ga^{66} + Cu^{64}$. The latest results, shown in Fig. 33, indicate a variation of less than 0.8 Mev across the alpha-particle beam which has the nominal energy of approximately 42 Mev. (J. A. Coleman and A. W. Fairhall)

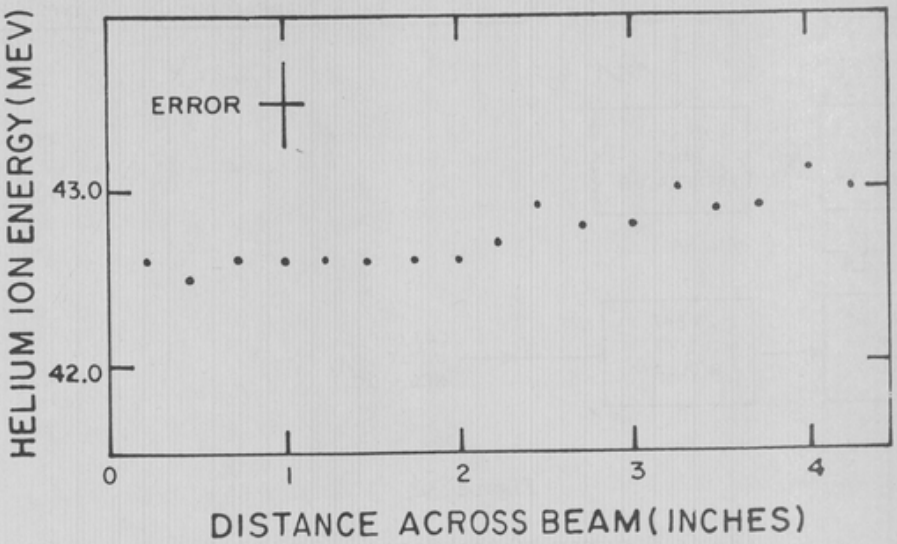

Figure 33

Variation of helium ion energy across the cyclotron beam. The indicated error refers to the uncertainty in relative energy determinations. The absolute energy is not precisely determined in this measurement.

---

1 N. T. Porile and D. L. Morrison, Phys. Rev. 116, 1193 (1959).

VIII. INSTRUMENTATION FOR RESEARCH

34. An Oscilloscope Plotting System for Particle Identification

A pulse-stretcher unit has been designed and constructed to make a dot plot of coincident pulses on an x-y oscilloscope. The principal motivation was the need for a particle identification system in which pulse heights from a "dE/dx" counter are plotted (vertical coordinate) vs. those from an "E" counter (horizontal coordinate). With such an arrangement, the oscilloscope screen, properly masked to reveal only the curve corresponding to one particle of interest, may be viewed by a photomultiplier, and used to excite a gating signal. The pulse-stretcher and oscilloscope combination has also been used in the study of the decay times for the scintillations excited in CsI(Tl) by various fast charged particles (see Sec. 35); in this case the fast (current) pulse from the photomultiplier is plotted vs. the slow (charge) pulse. Additional applications have been started and others are contemplated.

Transistors are used throughout the stretcher. The unit has two inputs, which accepts positive pulses ranging from 0.3 v to 18 v and from 5 v to 100 v, respectively. When the two stretched pulses are in coincidence, a positive signal is developed which feeds the z-axis of the oscilloscope to intensify the display. In addition, an external gating criterion can be imposed if desired on the z-axis intensification; this would be used, for example, in a fast-slow coincidence arrangement.

This chassis was built so that it could be also used as a slow coincidence unit (double or triple) without the stretching or intensifying features. A block diagram of the stretcher with a typical arrangement for using the system is shown in Fig. 34. (H. Fauska, R. West, and C. Zafiratos)

35. Identification of Particles by Pulse Shape Discrimination with CsI(Tl) Scintillators

Observations have shown that the decay time of the fluorescence excited in CsI(Tl) by a fast charged particle depends upon the nature of the particle as well as its energy, and it was suggested by Storey, Jack and Ward[1] that this effect could serve to identify the particle. They showed that the shape of the pulse depends upon the average ionization along the particle path. Becker[2] employed this effect in an investigation of the angular distributions of the B^{10} (d,α) Be^{8} reaction with energies between 0.58 and 1.50 Mev.

At this laboratory a study has been made of the possibility of using pulse shape discrimination. The decay times for alpha-particles and protons from the cyclotron, and for electrons with energies between 1 and 2 Mev have been measured. The crystal used was a CsI(Tl) cylinder 0.50 inch in diameter and 0.21 inch thick. It was optically coupled with Canada Balsam directly to the face of a 6810A photomultiplier. The electrical circuit used to power the photomultiplier was essentially that recommended by RCA for high sensitivity work, except that much larger capacitors were connected in parallel with the resistor across the last few dydynodes. The output of the photomultiplier was fed into a Model 535 Tektronix

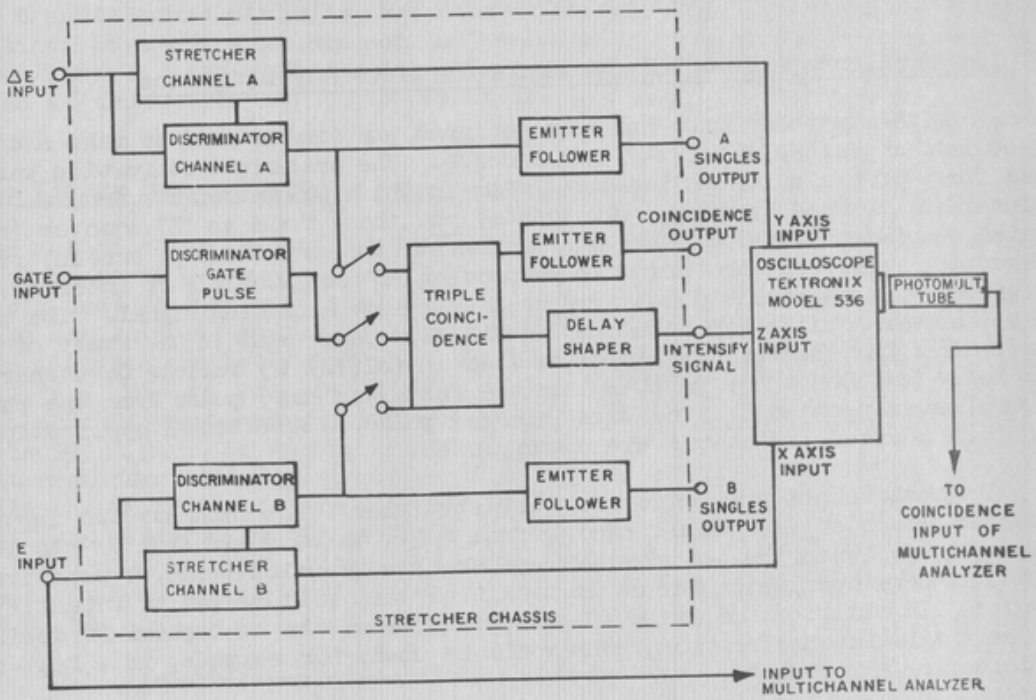

Figure 34

A block diagram of the stretcher with a typical set-up for particle identification.

oscilloscope with a CA-type plug-in unit, and the pulse traces were photographed with a Polaroid camera. The time constant of the output circuit was adjusted to minimize the statistical fluctuations of the pulses without affecting the decay-time of the pulse itself. Thus, the signal from the photomultiplier was proportional to current rather than total charge.

The results are shown in Table 35 and indicate quite clearly that CsI(Tl) crystals can be used for particle identification and energy determination for particles typical of reactions produced by the University of Washington cyclotron. The previous observations[1,2] that the decay-time for a given particle increases with energy can be seen clearly in the table. The decay times reported in Ref. 1 are also tabulated for comparison. (O. Larson, F. H. Schmidt)

---

1 R. S. Storey, W. Jack and A. Ward, Proc. Phys. Soc. (London) 72, 1 (1958).
2 R. L. Becker, Phys. Rev. 119, 3 (1960).

Table 35. Pulse Decay-Times

Particle	Energy (Mev)	Decay-Time (μsec)	Source of Particles
β (γ)	1 to E *	1.058 ± 0.020	Th decay series
β (γ)	E to 2.6 *	1.068 ± 0.029	Th decay series
p	20	1.041 ± 0.001**	α on polyethy. (30°)
α	6.09	0.424 ± 0.073	Bi^{212}
α	8.78	0.528 ± 0.005	Pb^{212}
α	33.5	0.765 ± 0.010	α on Teflon (30°)
β	0.66	0.70 ± 0.025	Ref. 1 data
p	2.2	0.52 ± 0.01	Ref. 1 data
p	8.6	0.595 ± 0.02	Ref. 1 data
α	4.8	0.425 ± 0.025	Ref. 1 data

* E denotes a value between 1. and 2.6 Mev.

** This number is the average for many pulses determined from a time exposure photograph.

36. Adder System for Particle Identification

A system based upon the addition of signals from conventional dE/dx and E detectors has been developed and used for particle identification in the study of (α, 2p) reactions (see Sec. 20). In this study the "dE/dx" counter must be thin and must give a fast signal. For this reason a scintillation counter was used with a 0.002"-thick plastic phosphor. A graph of the pulse height from the plastic counter vs. the pulse height from a succeeding CsI "E" detector is then found to be roughly linear, for incident protons and alpha particles of intermediate energy (E_p = 2.5 - 15 Mev). This fortuitous linearity arises primarily from the non-linearity in the response of plastic to heavily ionizing particles, which distorts the approximate hyberbola relating the energy losses into an approximate straight line.

By adding the signals from the two detectors, in an empirically determined proportion, it is possible to obtain separate groups for protons and alpha particles, whose pulse height is roughly independent of particle energy. An electronic unit was constructed for this purpose containing two particle identification channels (for the two coincident protons) and auxiliary coincidence circuits. Each identification channel has two amplifiers, a circuit which adds the outputs of these amplifiers, and a differential pulse height analyzer. The ratio of the amplifier gains is adjusted to give the best separation of protons and alpha-particles and the differential pulse height analyzer is set to accept only proton signals.

The performance of the system is seen in Fig. 36, where the output of one adding circuit is shown under conditions which are typical except for the absence of coincidence criteria. It is seen that proton and alpha-particle groups, which in this case represent broad continuous energy distributions, are reasonably separated.

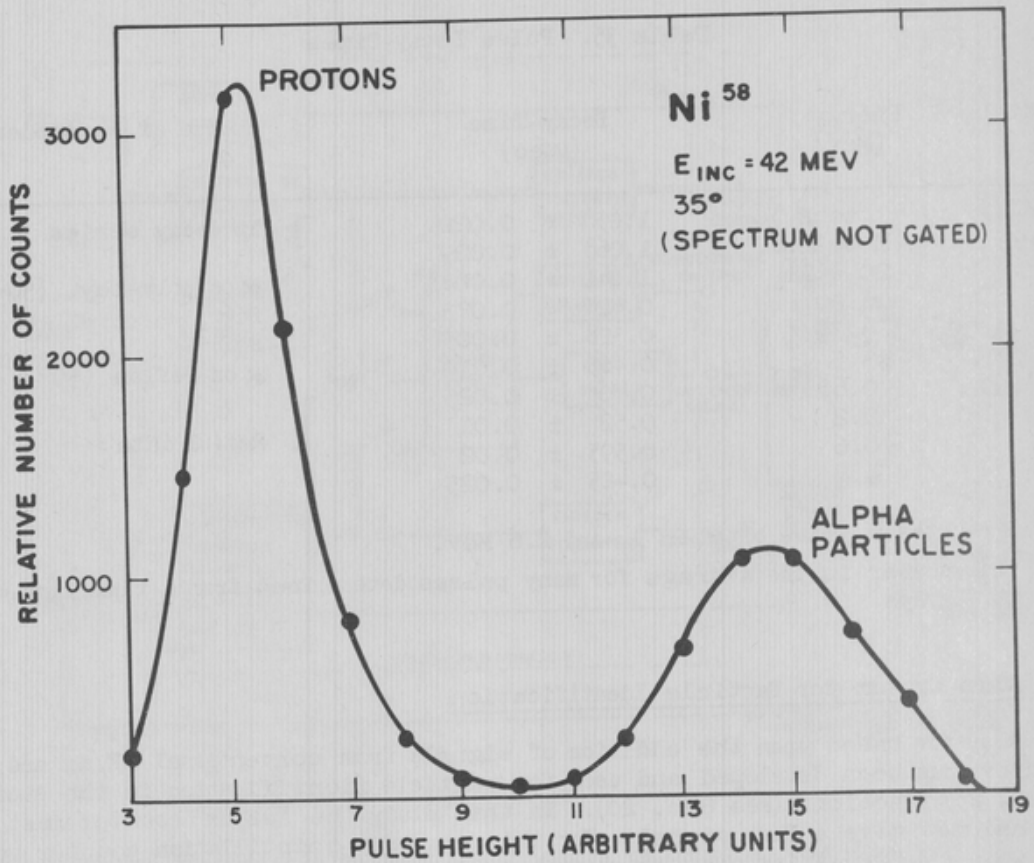

Figure 36

Pulse height distribution of signals from the adder circuit in the bombardment of Ni^{58} by alpha particles.

With a differential pulse height criterion which excludes all alpha particles, the efficiency for proton acceptance in the adder circuit was measured to be greater than 99 per cent for monoenergetic proton groups at energies ranging from 2.5 to 13.5 Mev, and is estimated to remain high up to about 20 Mev.

Most of the width of the groups in Fig. 36 is due to poor resolution in the signal from the very thin plastic. However, for protons above 15 Mev. the output pulse height becomes significantly larger than at lower energies, and the usefulness of this arrangement is limited to protons below about 20 Mev. Similarly, this system cannot distinguish deuterons from protons. However, in the present experiment it has been found that there are few high energy protons and it is inferred from evaporation calculations that there are few deuterons. Thus the addition system provides a suitable means of separating protons and alpha

particles. In general it can be a convenient tool in situations where the dE/dx detector uses an organic phosphor (which is non-linear) and where the demands for particle separation are relatively modest. (D. Bodansky, H. Fauska, and C. R. Gruhn)

37. A New Fast Scaler

A fast transistorized scaler, using a ring-of-five stage driven by a binary stage, has been designed and constructed. The ring-of-five stage was constructed following the design of Hutchinson et al[1], and has performed very well with a pair-pulse resolution time of 200 m sec. A fast discriminator and new binary stage were designed to feed the ring-of-five. The discriminator and the binary stage have a resolution-time of 100 mμsec, and will accept positive input pulses with amplitudes from 1 to 10 volts. The over-all unit has four decades with a meter read-out, and drives a register capable of handling fifty impulses per second. Any decade can also provide an audible "click" output for convenience in setting up equipment. (H. Fauska, R. Karns, and R. W. Peoples)

---

1 G. W. Hutchinson, R. Rubinstein, and W. H. Wells, Nuc. Instr. and Methods, 5, 167 (1960).

---

38. Multichannel Analyzers

A commercial 512-channel analyzer has been purchased and installed.

A two-dimensional analyzer, discussed in previous reports,[1] is under construction. The components necessary for one-dimensional operation have been completed and tested, and the analyzer has been in use as an ordinary one-dimensional 256-channel analyzer. The construction of the additional units necessary for two-dimensional operation is in progress. (H. Fauska, J. Heagney, and R. Mathews.

---

1 Cyclotron Research, University of Washington (1957), p. 50; (1959), p. 34; (1960), p. 45)

---

39. Miscellaneous Electronic Units

In addition to the electronic equipment discussed elsewhere in this report, a number of other electronic units were constructed during the past year. These units will be described briefly:

a. An electronic system, including a linear amplifier and differential pulse height analyzer, has been designed, constructed and installed, for use with a phototube beam monitor.

b. Charge sensitive, transistorized, preamplifiers for use with solid state detectors have been built and are in use. They work well for most purposes, but where there is need for very high resolution commercial vacuum tube units are being used instead. In addition, numerous conventional voltage sensitive preamplifiers have been constructed.

c. Power supplies have been built for phototube high voltage and solid state detector bias. The necessary B^+ and B^- supplies for units described elsewhere have also been constructed.

d. Multiplier circuits were constructed for particle identification, but, because of the success of the x-y oscilloscope system (Sec. 34) and the adder system (Sec. 36), these units have not been extensively tested. (H. Fauska)

40. The Heavy-Particle Magnetic Spectrometer Program

The heavy-particle magnetic spectrometer which was designed and completed last year[1] is now permanently installed in the cyclotron experimental area. It is driven by a hydraulic motor system which moves the 23 tons at a maximum of about 6 feet per minute along the circular tracks which maintain the magnet at a constant radial and vertical position with respect to the center of the scattering chamber. All electrical and water connections have been installed permanently in a manner which allows it to be moved freely without disrupting any of the circuits. Fig. 40-1 is a pictorial drawing of the magnet in the "cave" area which also shows its relation to the large scattering chamber. Experiments using the cyclotron beam as a source of energetic particles to study inelastic scattering processes are under way, and are described in Sec. 9.

Preliminary testing of the magnet with a Po^{210} source has been completed and has yielded important information: The optimum focal surface was found by measuring the line width as a function of the placement of the nuclear emulsion detector. Fig. 40-2 represents a typical set of such measurements for a given radius of curvature, that is, for a given field strength. We see from this graph that the aberrations produce a line width of about 0.12 cm. This implies that the resolution $(E/\Delta E)$ is greater than or equal to 1000. The shape of the peak, which has a low energy tail even with the best available source, indicates that with a monoenergetic source the line width would approach the ultimate resolution of about 2000, as determined from field mapping measurements.[1] The insert of Fig. 40-2 shows a typical peak obtained with the best Po^{210} source at the first order focal surface. Finally the absolute energy calibration of the spectrometer was determined by finding the parameters R_o and S_o which lead to the best fit to the theoretical equation for the focal plane[2]

$$S/R_o = 4.0344\,[\rho/(3-\rho^2)]\,[1 + .05425\,\rho^2 - 0.00619(1-\rho^2)^2 + 0.00125(1-\rho^2)^3 + 0.0027(1-\rho^2)^4] - 2.12663.$$

Here r is the distance from the center of curvature of the principal trajectory, R_o is effective radius of the magnet, $\rho = r/R_o$, and S is the distance along the plate from the $r = R_o$ point to the spectral line. The procedure was to measure S for several values of r, and then use this data in conjunction with the equation

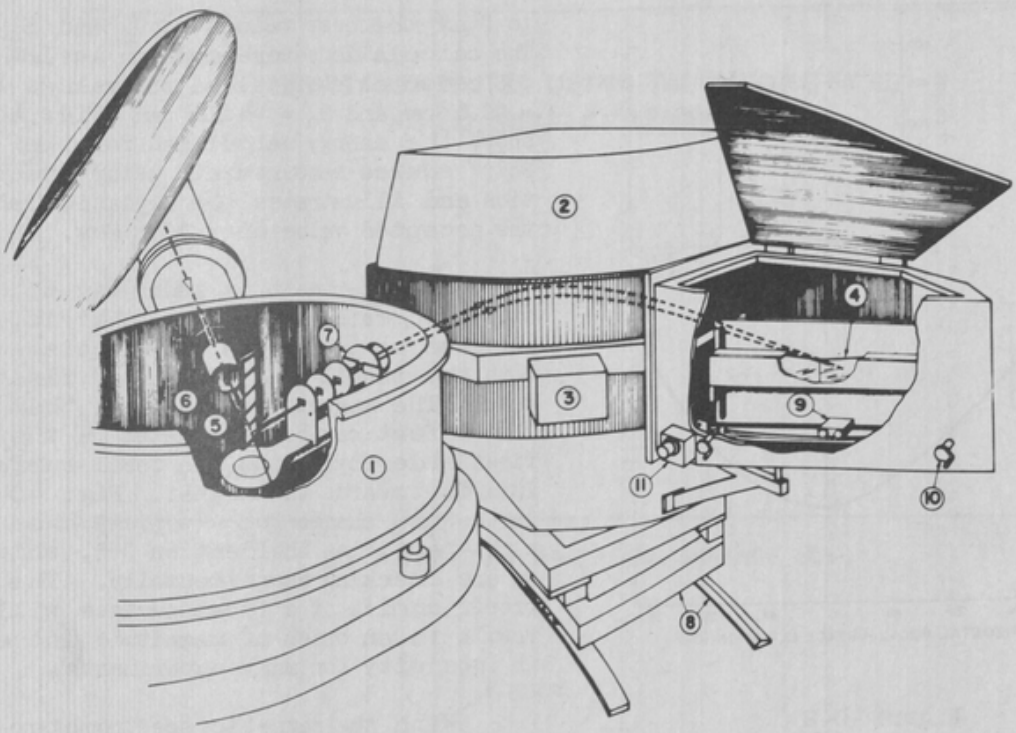

1. SCATTERING CHAMBER
2. MAGNET
3. PROTON RESONANCE
4. NUCLEAR EMULSION PLATES
5. TARGET
6. BEAM COLLIMATOR
7. COLLIMATOR AND ENTRANCE SLIT
8. CARRIAGE ON TRACK
9. COUNTER CART
10. FOCAL SURFACE ADJUSTMENT
11. COUNTER AND PLATE DRIVE

Figure 40-1

Pictorial view of heavy particle magnetic spectrometer in the experimental "cave" area of the University of Washington 60-inch cyclotron. At the present time the magnet can only be set at the experimental ports at 20°, 45°, 75°, 90°, 105°, and 120°. The numbers refer to: 1) scattering chamber, 2) magnet, 3) proton resonance, 4) nuclear emulsion plates, 5) target, 6) beam collimator, 7) collimator and entrance slit, 8) carriage on track, 9) counter cart, 10) focal surface adjustment, 11) counter and emulsion plate drive.

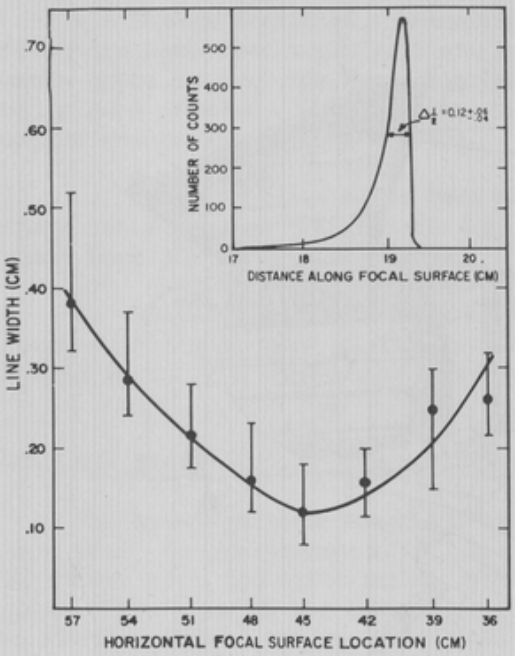

Figure 40-2

Plot of the measured line width as a function of the emulsion detector position from a given reference position. All widths for above curve were measured at a given radius, r_o, of curvature. This was done for five different r_o spanning the surface to precisely locate the surface of best first order focus. Insert shows a typical line at a position of best focus (i.e., at the minimum of the curve).

to find the best values of R_o and S_o. The calculations were made on an IBM 650 computer and yielded the values R_o = 90.6 cm and S_o = 74.16 cm. Fig. 40-3 shows the energy calculated for the Po^{210} source measurements using the equation and illustrates the deviation about the accepted value of 5.3056 Mev.

An experiment is under way to study kinematic broadening, that is, the increase of the line width associated with the recoil of a nucleus of finite mass. The magnet theory[3] shows that this effect can be eliminated in the first order by moving the focal surface inwards towards the magnet. Fig. 40-4 shows this change for a typical case of alpha-particles incident on C^{12}, which we are checking experimentally. The proper choice of a focal surface will result in an order of magnitude increase in intensity for many experiments.

With the magnetic spectrometer now available for research with the cyclotron, many new experiments requiring high resolution will become feasible. A resolution of 0.30 per cent for a four-hour cyclotron run was obtained for alpha-particles scattered from zinc. Junction counters now available give a typical resolution of 0.7 per cent. Thus, from the standpoint of resolution alone, the magnet is superior to any other technique by a factor of two. It now seems that this high resolution coupled with the elimination of almost all unwanted background should make the spectrometer a powerful tool for the future except for experiments in which detailed angular distributions are needed. (W. Brandenberg, D. Hendrie, and D. K. McDaniels)

---

1 Cyclotron Research, University of Washington (1960), p. 45.
2 S. F. Zimmerman, Jr., Focussing Properties of a High Resolution Magnetic Spectrograph, M.S. thesis, Mass. Inst. of Tech. (1955).
3 D. K. McDaniels, Nuclear Reaction Studies at Intermediate Energies, Ph.D. thesis, University of Washington (1960).

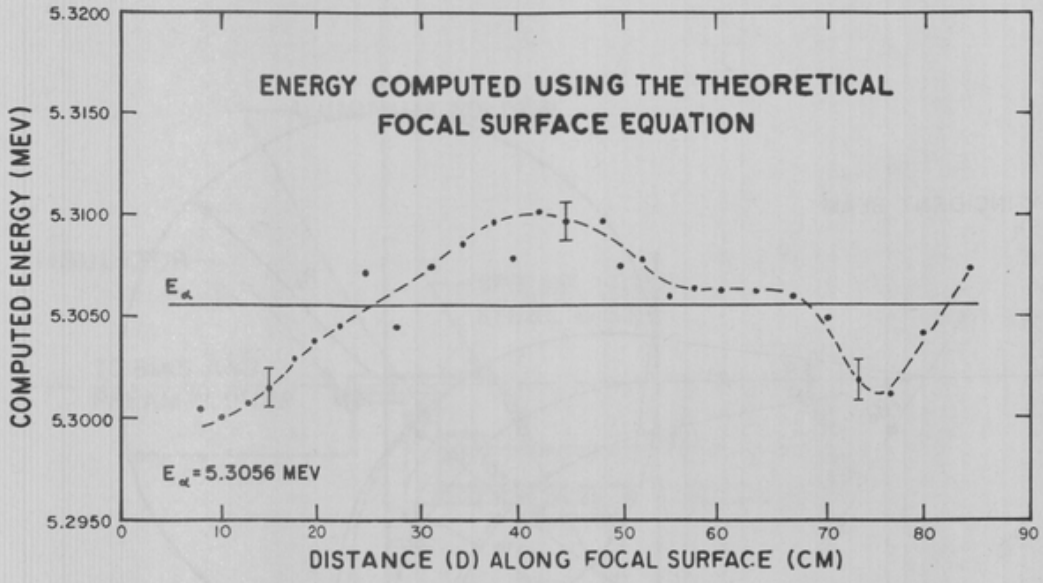

Figure 40-3

Plot of the energy computed for the Po^{210} alpha source measurements using the theoretical focal surface equation and the IBM 650 computer program. The solid line represents the accepted value of 5.3056-Mev.

41. Development of Solid State Detectors

High resistivity (12,000 - 26,000 ohm-cm) p-type silicon was used in making junction detectors which stop 42-Mev alpha-particles. The silicon surface was lapped with fine grit carborundum, etched with CP_4 at zero temperature and doped with donor impurities at 930°. Spring-loaded wires provided the electrical connections to the detector (See Fig. 41-1).

The pulses from the detector were fed into a charge-sensitive preamplifier and analyzed with a 20-channel pulse height analyzer. The linearity curve (Fig. 41-2) shows that the depletion region is thick enough to stop at least 42-Mev alpha-particles when the voltage bias equals 285 volts. The energy resolution (full-width at half-maximum) was about 0.6 per cent for 40 Mev alpha-particles. This is similar to the resolution of a solid state detector furnished by R.C.A.[1] (Fig. 8-1) (I. M. Naqib, J. P. Toutonghi,* and R. W. Williams*)

---

1 R.C.A. Victor Company, Ltd., Montreal, Canada.

* Mr. Toutonghi and Prof. Williams are members of the High Energy Physics group in the Department of Physics, University of Washington

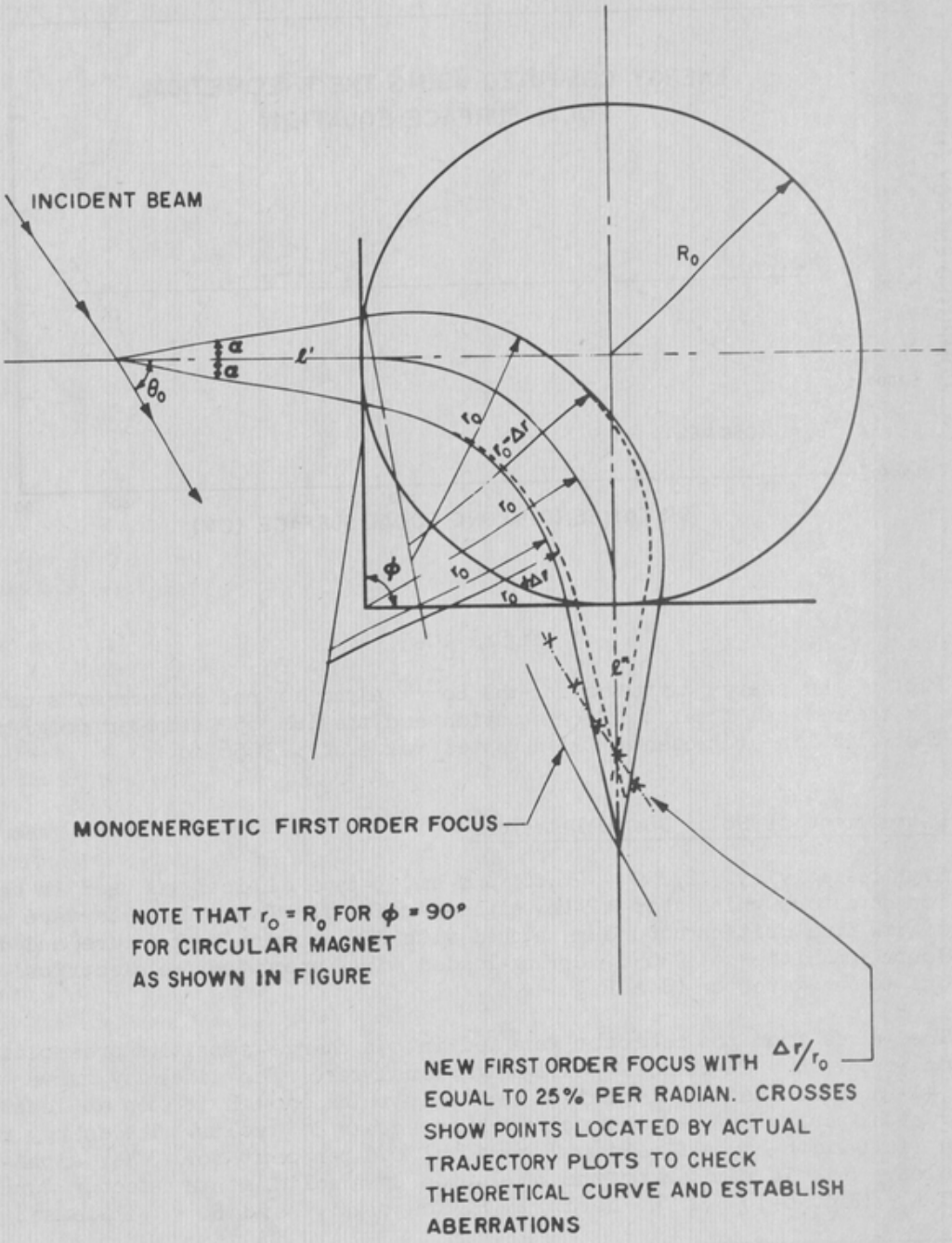

Figure 40-4

Nomenclature and paths of particles used in locating the first order direction focal surface with kinematical broadening present.

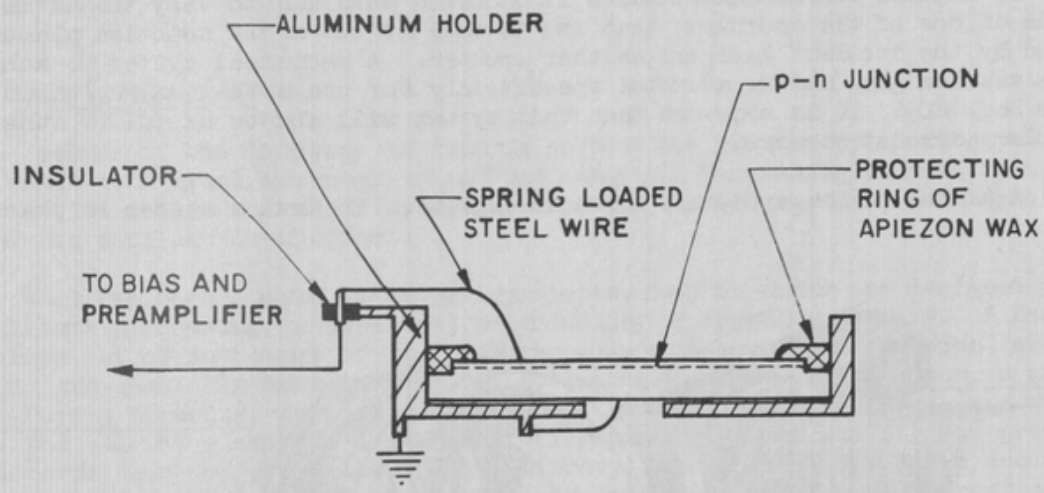

Figure 41-1

p-n junction detector mounted in an aluminum holder.

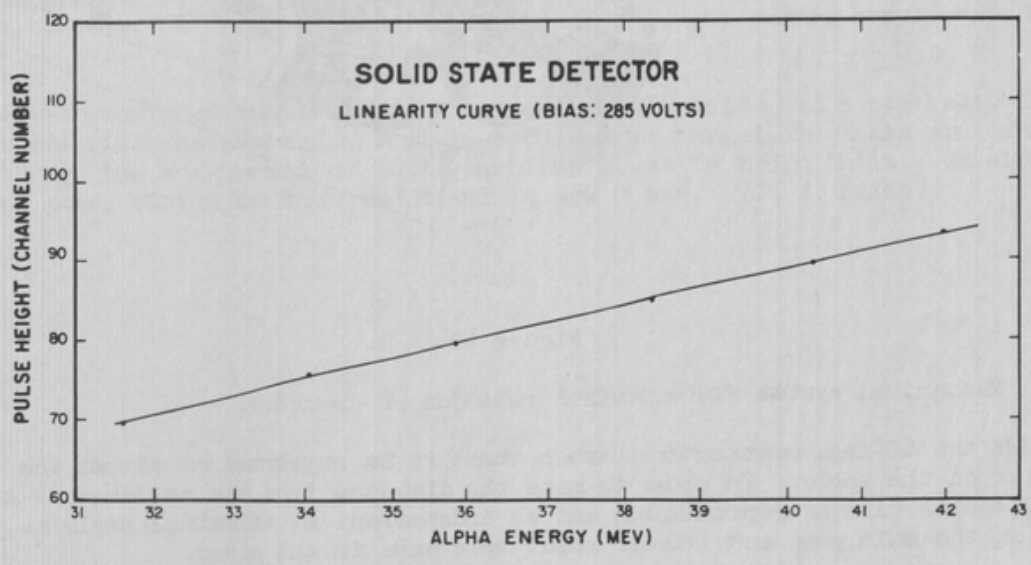

Figure 41-2

Linearity curve for solid state detector. The alpha-particles were scattered by C^{12}. The alpha-particle energy was varied by changing the scattering angle.

42. Mechanical System for Azimuthal Rotation of Counters

In angular correlation studies it is often desirable to vary the azimuthal angle of one of the counters; that is, to move it out of the reaction plane defined by the incident beam and another counter. A mechanical system to achieve this was designed and constructed specifically for use in the (α, 2p) studies (see Sec. 20). It is expected that this system will also be useful in other angular correlation work.

A sketch of the system is shown in Fig. 42. The entire system is placed

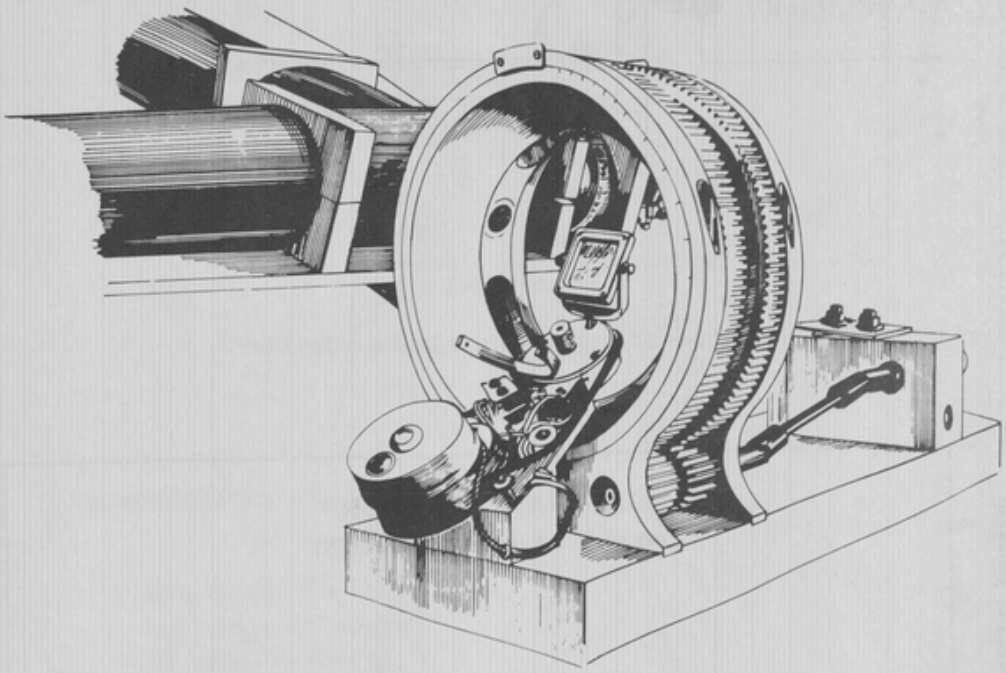

Figure 42

Mechanical system for azimuthal rotation of counters.

inside the 60-inch scattering chamber where it is supported on either the upper arm or on the table. In order to make the distance from the collimators to the beam center line as reproducible and as independent of azimuthal angle as possible, the main gear and counter mount were made in one piece.

The minimum polar angle with respect to the incident beam is 30°. The azimuthal angle may be varied from 45° below the reaction plane on one side of the beam to 45° below the plane on the other side, a total of 270°. The azimuthal angle is controlled either remotely from the counting room or at the

mechanism and may be read either remotely to within 0.3° using a resistive bridge circuit or at the mechanism to within 0.1° with a calibrated vernier scale. (C. R. Gruhn)

43. Target Materials

Because of the diversity of targets used in the laboratory an attempt has been made to collect and organize all the materials for making targets in a way that will minimize the use of cyclotron time for testing new target materials and avoid duplication of effort.

Work has been started on several projects, most of which are designed to facilitate purchasing, preparation, and handling of target materials. A fairly complete set of catalogues of the major suppliers of separated isotopes, metal foils, and chemicals has been obtained including the UCRL Report, Sources of High-Purity Elements, which lists suppliers, purity, unit cost, form, and delivery time for all the elements. A permanent file of target availability and procurement cards has been established in the library. These cards are filed according to the atomic number of the element and give information about the target material, thickness, isotopic purity, and methods of preparation. A reference to the original article is also given. This file is designed so that a card may easily be filled out if an interesting target-making technique or a new supplier of bizarre materials is mentioned in a paper. This file includes information on: 1) General target-making techniques cross-filed to the elements to which these techniques are applicable, 2) backing materials including instructions for their use and their chemical and physical properties, 3) liquid target techniques, 4) gas target techniques, and 5) target thickness measurement references. A collection of reprints of articles dealing with the techniques of target-making supplements this file.

A well-equipped target-making area has been set aside and a central pool of target materials established. A gauge to determine target thickness and uniformity through the measurement of alpha-particle pulses is being built. An electroplating power supply has been built and is now in use. (P. A. Kelsh)

APPENDIX

44. Statistics of Cyclotron Operation

Loss of operating time during the year was principally associated with: (1) burning-out of the motor of the cyclotron magnet motor-generator set; (2) replacement of the copper-plated iron loop insulator seal plates with aluminum plates; and (3) draining, cleaning and replacing the oil in the cyclotron magnet cooling system. The disposition of the time available for cyclotron operation during the year is given in Tables 44-1, 44-2, and 44-3 which are self-explanatory.

Table 44-1. Division of Cyclotron Time Among Activities

Activity	Time	
	Hours	Per Cent
Normal Operation	4901	70.6
Setup of Experiments	699	10.1
Cyclotron Testing	195	2.8
Scheduled Repairs and Modifications	132	1.9
Unscheduled Repairs	557	8.0
Failure of Experiment Equipment	76	1.1
Unsatisfactory Cyclotron Operation	71	1.0
Experiments Using No Beam	189	2.7
Unrequested Time	119	1.7
Visitors	7	.1
	6946	100.0

Table 44-2. Division of Normal Operation Time Among Major Facilities

Activity	Time	
	Hours	Per Cent
60-Inch Scattering Chamber	3833	55.2
24-Inch Scattering Chamber	251	3.5
Target Box Bombardment by Laboratory Personnel	701	10.1
Target Box Bombardment for Others	81	1.2
Tests	41	0.6
	4901	70.6

Table 44-3. Division of Normal Operation Time Among Projectiles

Projectile	Time	
	Hours	Per Cent
Alpha particles	3402	69.4
Protons	1420	29.0
Deuterons	79	1.6
Total	4901	100.0

45. Bombardments for Outside Investigators

During the year bombardments were requested by and performed for a number of outside investigators. These bombardments are summarized in Table 45. These bombardments were for the continuation of experiments already in progress which were listed in the previous report.[1]

Table 45. Operation Time for Outside Investigators

Investigator	Time	
	Hours	Per Cent
Washington State University	52.8	0.76
University of Colorado	3.9	0.05
Ohio State University	18.6	0.27
Boeing Airplane Company	6.1	0.09
Total	81.4	1.17

1 Cyclotron Research, University of Washington (1960), p. 51.

46. Building Additions

In its unfinished condition the upper floor of the cyclotron building addition provided temporary housing for the beta-ray spectrometer laboratory, a carpenter and cabinet shop, and various minor facilities used in connection with current experiments. This area has now been finished, and contains a conference room, a library, a drafting room, the beta-ray spectrometer laboratory, a student drafting and calculating room and a student office room.

47. Advanced Degrees Granted

It is planned that in this and in each future progress report there will appear a list of the individuals who have, during the period covered by the report, been granted, by the University of Washington, advanced degrees, which are based in part on original research carried out at the Cyclotron Laboratory. Since such a list has not been given previously, there is given below a compilation of all degrees of this category awarded up to this time. Following the name of the individual is the designation of the degree and the title of the thesis submitted in partial fulfillment of the requirements for the degree. At the present a thesis is not required for the M.S. degree.

Academic Year 1950-51

Joseph O. Stenoien: M.S. Measurements and Shaping of the Magnetic Field of the University of Washington Cyclotron.

Harvey E. Wegner: M.S. Measurements and Shaping of the Magnetic Field of the University of Washington Cyclotron.

Academic Year 1951-52

Glen Keister: M.S. An analysis of the Radioactive Decay of Cesium-134.

Philip V. Livdahl: M.S. Initial Operation of the University of Washington 60-Inch Cyclotron.

Academic Year 1952-53

Glen Keister: Ph.D. The Second-Forbidden Beta-Spectra of Co^{60} and Sc^{46}.

Wesley Robinson: M.S. The Energy Distribution in the Ion Beam of the University of Washington Cyclotron.

Harvey E. Wegner: Ph.D. Elastic Scattering of Alpha Particles by Heavy Nuclei.

Academic Year 1953-54

John Coffin: M.S. Evaluation of a Time-of-Flight Method for Determining the Energy Loss of Protons in Materials.

Academic Year 1954-55

Donald J. Farmer: Ph.D. The Annihilation of Positrons in Flight.

Academic Year 1955-56

Robert L. Brock: Ph.D. An Attempt to Observe the Lyman-Alpha Line of the Positronium Spectrum.

Clifford T. Coffin: Ph.D. Angular Distributions in Fission Produced by Alpha Particles and Deuterons.

J. M. Robin Hutchinson: M.S. The Exploration of a Recoil Technique for (α, n) Reactions.

Donald D. Kerlee: Ph.D. A Study of Nuclear Structure Through Alpha-Particle Scattering.

John R. Penning, Jr.: Ph.D. The Decay of Neon-23.

Academic Year 1956-57

Monte P. Hickenlooper: M.S. Angular Anisotropies of Thorium Fission Fragments (40 Mev Alphas).

Academic Year 1957-58

James B. Ball: Ph.D. Radioactive Capture of Alpha Particles and Deuterons at Energies up to 40 Mev.

Samuel F. Eccles: Ph.D. The 7.65-Mev Excited State in C^{12}.

Reilly C. Jensen: Ph.D. Mass-Yield Distributions of the Fission Fragments from Particle-Induced Fission of Ra^{226}.

Martin E. Rickey: Ph.D. A Study of the Nuclear Reactions $C^{12}(\alpha,p)\ N^{15}$ and $N^{14}(d,\alpha)\ C^{12}$.

Paul C. Robison: Ph.D. Angular Distributions for Elastic and Inelastic Scattering of Alpha Particles by B^{10}, B^{11}, and S^{32}.

Gail B. Shook: Ph.D. Angular Distributions and Alpha-Gamma Angular Correlations for Alpha Scattering by C^{12}, Mg^{24}, and Ca^{40}.

Avivi I. Yavin: Ph.D. Elastic and Inelastic Scattering of Alpha Particles from C^{12}, N^{14}, O^{16}, A^{40}, and He^{4}.

Academic Year 1958-59

George H. Bouchard, Jr.: M.S. Study of the 30-43 Mev He-Ion Induced Formation of Be^{7} From Al^{27}, O^{16} and Other Light Elements.

Henry Crew: M.S. A Transistorized Scaler.

Robert K. Cole: Ph.D. A Coincidence Study of Proton Emission in Alpha Particle Bombardment of Nickel and Iron.

Edward F. Neuzil: Ph.D. A Study of the Alpha Particle Induced Fission of Some Elements Lighter Than Polonium.

Academic Year 1959-60

John C. Hopkins: Ph.D. The Longitudinal Polarization of Oxygen-14 Positrons.

Paul Meyer: M.S. Precision Magnetic Field Adjustments of the External Beam Analyzing Magnet of the University of Washington Cyclotron.

William J. Nicholson, Jr.: Ph.D. Measurements Relating to the Height of the Fission Barrier in Elements Lighter Than Thorium.

Hugh Nutley: Ph.D. The Decay of Silver-104.

Jan E. Stroth: M.S.

Academic Year 1960-61

Patricia A. Kelsh: M.S. Low Energy Alpha Particle Fission of Rhenium.

Albert J. Lieber: Ph.D. An Investigation of the Nuclear Reactions C^{12} $C^{12}(\alpha,p)N^{15*}$, $Al^{27}(\alpha,p)Si^{30*}$, and $P^{31}(\alpha,p)S^{34*}$ at 42 Mev.

David K. McDaniels: Ph.D. Nuclear Reaction Studies at Intermediate Energies.

Richard E. Wilson: Ph.D. Angular Distributions of Some Selected Fission Fragments.

CYCLOTRON PERSONNEL, 1960-1961

Faculty

David Bodansky, Associate Professor
Arthur W. Fairhall, Associate Professor
George W. Farwell, Professor[1]
James B. Gerhart, Assistant Professor
I. Halpern, Professor
Fred H. Schmidt, Professor
John F. Streib, Associate Professor

Cyclotron Research Staff

Sheau-Wu Chen, Research Instructor[2]
David K. McDaniels, Research Instructor
Taku Matsuo, Research Instructor
Ted J. Morgan, Research Associate Professor; Supervisor, Cyclotron

Graduate Student Predoctoral Associates

Francis Bartis
Darrell Drake
Charles R. Gruhn
Albert Lieber[3]
Isam Naqib
William J. Nicholson, Jr.[4]
Chris Zafiratos

Graduate Student Research Assistants

Physics

Werner Brandenberg
H. David Glenn
Joseph Heagney
David Hendrie (N.S.F. Fellow)
Wojciech Kolasinski
E. Roland Parkinson
Frank Perry
Joseph Ramus[5]
Gurnam S. Sidhu
Frederick Slee
Jan E. Stroth[6]
Richard West

Chemistry

Joseph A. Coleman
Charles O. Hower
Richard Wilson[7]

Full-Time Technical Staff

Machine Shop

Harvey Bennett, Foreman
Norman E. Gilbertson
Charles E. Hart
Floyd E. Helton
Gustav Johnson
Bernard Miller, Assistant Foreman
Byron A. Scott
Allen L. Willman

Electronic and Electrical

Laverne Dunning
Robert B. Elliott
Harold Fauska, Senior Physicist, Research Electronics Supervisor
Russell E. Karns, Jr.
Richard Matthews
Robert L. McKenzie
John W. Orth, Assistant Supervisor

Design and Drafting

Gerald Bartley
Peggy Douglass
Ralph Flaaten, Engineer
Clyde Louk

Cyclotron Operators

Donna M. Brown
Nicola I. Carlson[8]
Georgia Jo Rohrbaugh[9]

Others

Patricia A. Kelsh, Radiochemist
Ann E. Rutter, Secretary

Part-Time Technical Staff

Cyclotron Operators

Roy J. Peterson
John Turneaure

Student Helpers

Ralph Christofferson
Merlyn J. Flakus
Kyum-Ha Lee
Carol Lewis
Patricia Rice
Akiko Yamanouchi

Others

Chester Chen, Draftsman[8]
Catherine Cowles, Secretary[8]
Sharon A. Gill, Clerk-Typist
Jewel Kerbaugh, Secretary-Typist[8]
Gail A. Lotto, Clerk-Typist[8]
Ralph W. Peoples, Jr., Electronic Technician
William Stolcis, Stores Manager

---

1 On leave at Institute for Theoretical Physics, Copenhagen.
2 Now at Cavendish Laboratory, Cambridge, England.
3 Now at Convair, San Diego, California.
4 Now at Watson Research Laboratory, New York.
5 Employed during the summer only.
6 Now at San Jose State College, San Jose, California.
7 Now at Argonne National Laboratory, Illinois.
8 Terminated.
9 Now on leave.

List of Publications

The following articles, originating in this laboratory, were published during the year ending June 15, 1961. Several of them appeared in periodicals which were dated prior to that period, but which were distributed during that period:

"The Evaporation of Protons from Rapidly Rotating Nuclei," D. Bodansky, R. K. Cole, W. G. Cross, C. R. Gruhn, and I. Halpern, Proceedings of the International Conference on Nuclear Structure, Kingston, p. 749 (1960).

"Fixed Frequency Cyclotron Operation with a Regulator for Dee-Voltage Stabilization," H. Fauska, J. W. Orth, and F. H. Schmidt, Nuclear Instruments and Methods, 10, 73 (1961).

"Longitudinal Polarization of O^{14} Positrons," J. C. Hopkins, J. B. Gerhart, F. H. Schmidt, and J. E. Stroth, Phys. Rev. 121, 1185 (1961).

"The Use of Oxygen-14 in the Study of Positron Polarization in a Fermi-Type Transition," F. H. Schmidt, J. B. Gerhart, H. Bichsel, J. C. Hopkins, and J. E. Stroth, Paper read at International Conference on Radioisotopes, Copenhagen, Sept. 1960. Abstract appears in International Journal of Applied Radiation and Isotopes, 9, 175 (1960).

"Apparatus for Methane Synthesis for Radiocarbon Dating," A. W. Fairhall, W. R. Schell, and Y. Tahashima, Rev. Sci. Instr. 32, 323 (1961).

"The Radiochemistry of Beryllium," A. W. Fairhall, National Academy of Science, National Research Council, Nuclear Science Series, No. 3013 (1960).

"The Half Life of O^{14}," D. L. Hendrie and J. B. Gerhart, Phys. Rev. 121, 846 (1961).

"The Decay of Ag^{104} and Levels in Pd^{104}," H. Nutley and J. B. Gerhart, Phys. Rev. 120, 1815 (1960).

"Alpha Particle Excitation of Quadrupole and Octupole Surface Modes in Ti, Fe, Ni, Zn and Sr," D. K. McDaniels, J. S. Blair, S. W. Chen, and G. W. Farwell, Nuc. Phys. 17, 614 (1960).

"Diffraction Analysis of Elastic and Inelastic Scattering by Magnesium," J. S. Blair, G. W. Farwell, and D. K. McDaniels, Nuc. Phys. 17, 641 (1960).

"Kinematic Effects in Target Thickness Corrections," I. Naqib and D. K. McDaniels, Rev. Sci. Instr. 31, 1358 (1960).

The following invited papers were presented by members of the cyclotron group during the year ending June 15, 1961:

"Evaporation of Particles from Rapidly Rotating Nuclei," I. Halpern, Paper presented to the American Physical Society meeting, Berkeley, December, 1960.

"Persistent Puzzles about the Nuclear Fission Process," I. Halpern, paper presented to the American Chemical Society meeting, St. Louis, March, 1961.